ASIAN DISASTER REDUCTION CENTER

FINAL REPORT

"Earthquake Building Risk Assessment in Sana'a City, Yemen "

Prepared by:

Moneer Abdulla Al-Masni

Seismological and Volcanological Observatory Center (SVOC)

Ministry of Oil & Minerals

VISITING RESEARCHER (ADRC)

Aug. to Nov. 2012 (FY2012A)

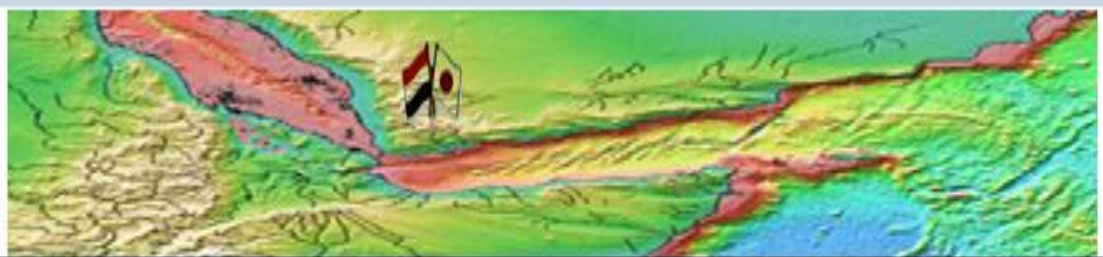

Disclaimer

This report was compiled by an ADRC visiting researcher (VR) from ADRC member countries.

The views expressed in the report do not necessarily reflect the views of the ADRC. The boundaries and names shown and the designations used on the maps in the report also do not imply official endorsement or acceptance by the ADRC.

Table of Contents

1. Significant and Background:

Earthquakes are one of the most dangerous, destructive and unpredictable natural hazards, which can leave everything up to a few hundred kilometers in complete destruction in seconds.

Reducing urban earthquake risk involve three stages, evaluation, planning, and implementation. This research focused on the risk evaluation stage which considers very important stage for doing the next stages. As well as, this stage is necessary needed for improvement disaster management system in Yemen which have attention only on post disaster response.

Sana'a city in Yemen is one of the oldest cities in the worlds, which has different forms of building built with different types of materials. In the present work, the old and new forms of building construction and the building materials are used for damage analysis.

Sana'a city has high priority attention due to several considerations. It is represent the capital of Yemen, contain one of the oldest city in the world and housed more than 1,750,000 people(Central Statistical Organization,2005).

During the last tow decades, the city has been growing and expanded by more than 3 times its area in 1982, in both vertically and horizontally to provide housing, business and man-mad structures .

On the other hand, historical records mentioned that it was subjected by destructive earthquakes in the past periods (742 BC,1644 and 1908) with equivalent magnitudes between (M 4.0- M 6.0). As well as, it was not far from impacts of the strongest earthquake (Mw6.2) which occurred in Dhamar in 13, Dec.,1982 ,70km south Sana'a, caused a big damage in livelihoods and property in Dhamar and large scale fractures in Dhamar and Sana'a basins.

Further more, many of small earthquakes of magnitude less than 4.2 occurred on the period(1995-2012) highly felt by most of peoples because, Sana'a city situated on a thick

soft alluvium sedimentary basin that acting to amplify the seismic ground motion and make weak buildings more vulnerable to damage caused by moderate earthquakes.

For estimation the potential damage of an expected future earthquake, theoretical estimation is performed by combining the seismic intensity distribution that is estimated for the adopted earthquake with the inventory of the structures and infrastructure of the city. This combination is performed using vulnerability functions that are developed to reflect the seismic behavior of the structures and infrastructure found in the city.

2. Aims of Research:

In the absence of attention to the pre-disaster planning, the current research aims to assess building damage prediction at Sana'a city by developing historical earthquake scenarios and investigate the behavior of buildings during destructive earthquakes. As well as to provide the a common basis for governmental and other agencies to rising the preparedness and planning the best emergency response at city level.

3. Description of study area

3.1 Geographical Location and Topography:

The city is situated on Sana'a basin which is considered one of the most important deposits basins in the central highlands. The basin located at the area between (44 º 10ˋ,44º 37ˋE) & (15 º 10ˋ,15 º 28ˋN) , reach to 2300m above sea level and covers an area estimated to 3200km^2. Sana'a basin is characterizing by tectonic valleys features which is surrounded by mountains of many breaking edges, flow propellers, faults and volcanic cones forming dikes and ash overlaying alluvial sediments. Figure.1 shows location and (3D) view proposed by satellite image show geomorphology of Sana'a basin.

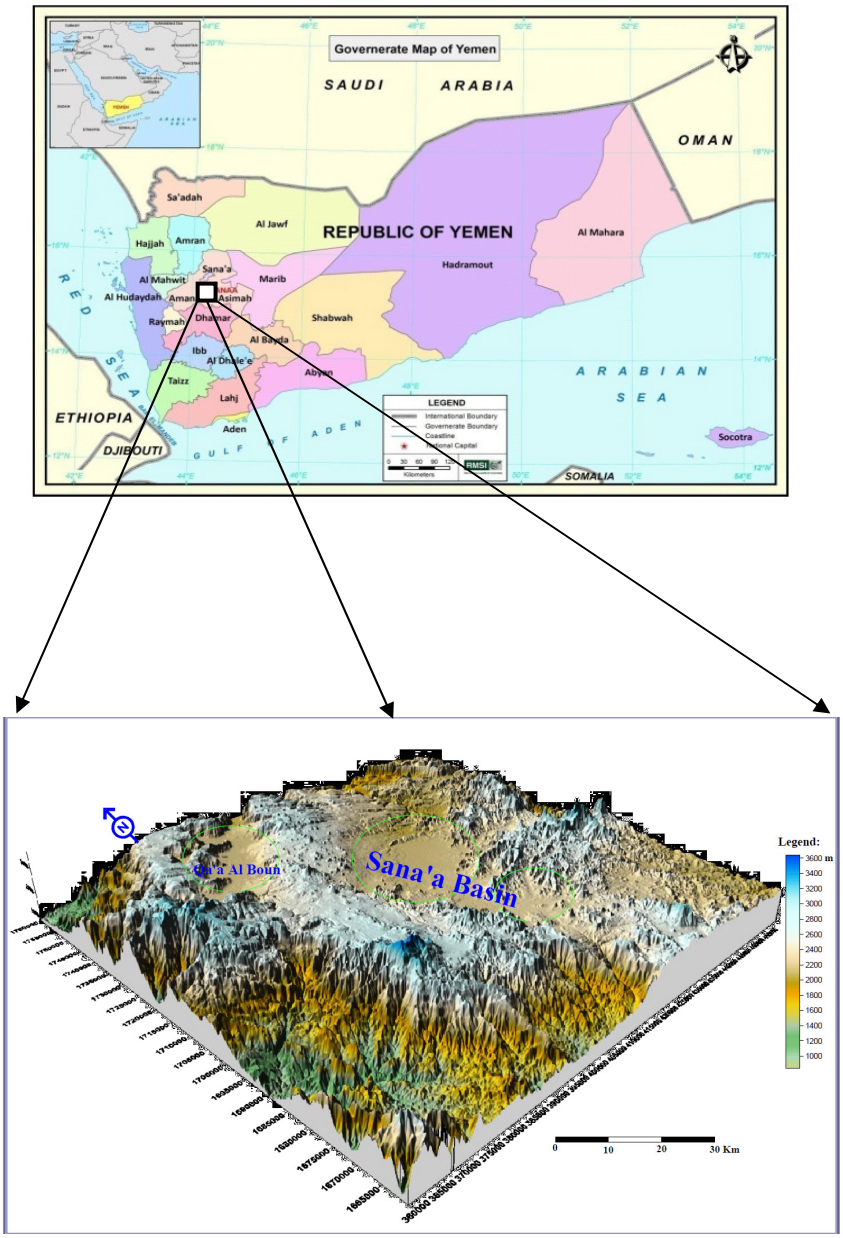

Figure.(1) Location and (3D) view proposed by satellite image show geomorphology of Sana'a basin

3.2 Geology and Tectonic

The geology of Yemen is related to the regional geology of the Arabian Peninsula, which is part of Arabian-Nubian plate in a structural sense. In late Pre-Cambrian, the Arabian shield joined to the African shield by plate collision. During the Paleozoic-Mesozoic time the Pre-Cambrian basement is depressed and an extensive marine platform developed on the northeastern part of the Arabian shield. Both the plates drifted to the north east

closing the Tethyan seaway. In mid Tertiary period, the Afro-Arabian plate collided with the Eurasian plate forming the Zaggros Mountains and the Iranian fold belt. At the same time, the Arabian plate was detached from the African plate by the Aden-Red Sea rift.

The morphological features of the country, formed largely as a result of the tectonic and volcanic activities during the Tertiary, were modified to some extent during the Quaternary period. The overall geological structure of Yemen is dominated by the Precambrian Arabian Shield in the western part of the country and an extensive and thick cover of Phanerozoic sub-horizontal sediments further east. Figure 2, shows general geological map developed on a 1:1 million scale. The geological settings of Yemen are characterized by the wide variety of main rock units, which range from Precambrian to Quaternary. In the southern and western regions of Yemen, the Precambrian crystalline basement and its older sedimentary cover are uplifted and partly exposed (Arabian Shield-zone). The Tertiary volcanic is also associated with westerns region. Whereas the eastern part of Yemen consists mainly of Paleozoic, Mesozoic and Cenozoic sediments.

In the particular of Sana'a basin geological, there are five significant rock Formations outcropped in the surface of Sana'a basin. The first, is Al- Tawilah (Cretaceous-Paleocene) Sandstone formation, outcrops to the west and north east parts of the Sana'a basin. The second, is Amran Limestone Formation, outcrops to north of Sana'a basin. The third, is Yemen Volcanic (Tertiary Stratoid) Formation, mostly Ryolitic Yellow Tuff and Basalts, outcrops and widely spread in west and south east of study area. The fourth, is Quaternary Basalt consists of massive and sheet rock outcrops in the center and northwest of Sana'a basin. Quaternary volcanic cones forming dikes and ash overlaying Al-Tawila sandstone. The fifth, is Quaternary thick alluvium sediments plain, outcrops in the middle of the basin and covered 500km^2.

In respect to tectonic features in Sana`a basin, Al- Ubaidi and Al-Kotbah (2003), reported that three main tectonic fracture trends was recorded in the basin. The first

one is NE-SW which represent the old trend and probably rejuvenated from Hajaz Orogeny, the second trend is NW-SE which represent the most dominant fractures and major faults results in the formation of Jurassic basins and were accompanied with compressional strike slip and thrust faults which rejuvenated from Najid fault system, and the third and youngest trend is E-W which coincides with the trend of the Gulf of Aden. However, the old fractures of Jurassic and Cretaceous are obscured by the youngest trends of the Red Sea and the Gulf of Aden where all localities are highly dissected by these two trends. Figure. 3. shows the surface lithology and structures of Sana'a basin.

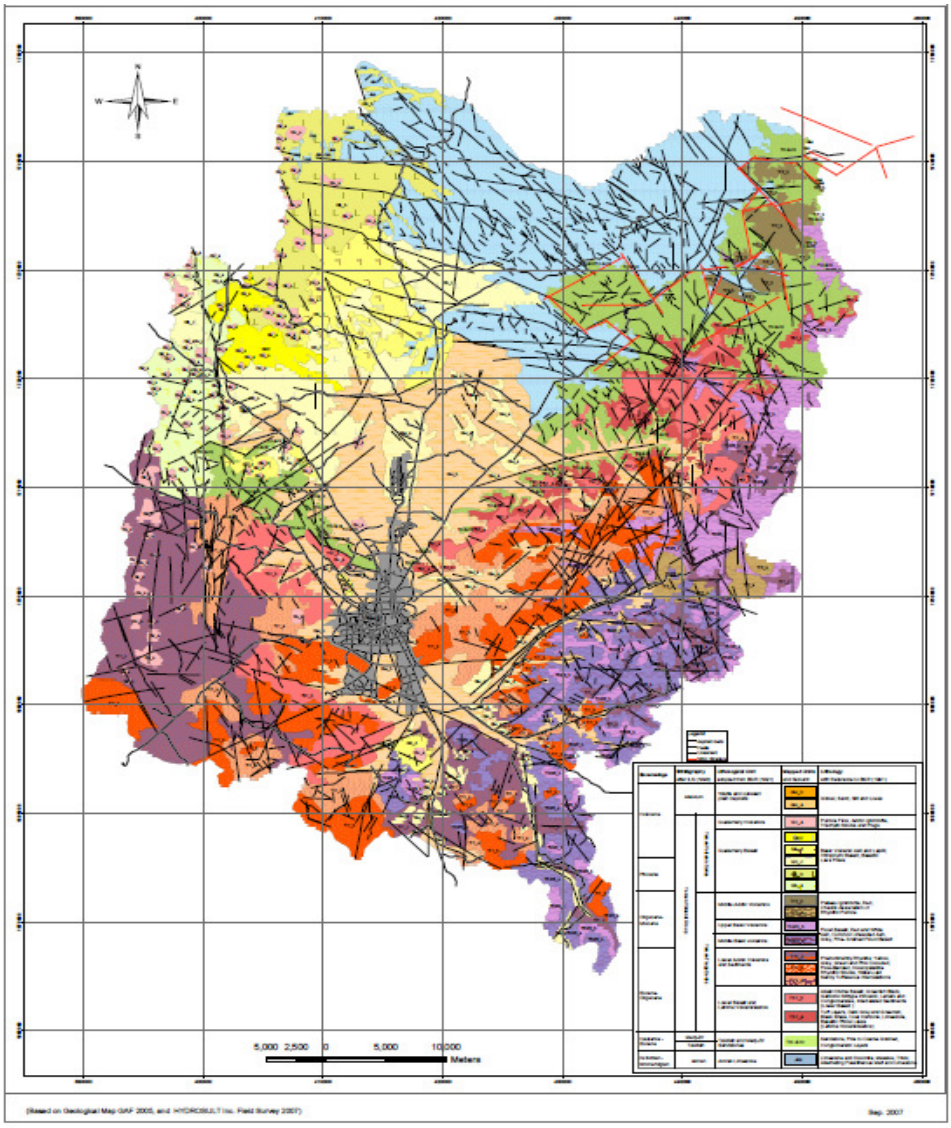

Figure.(3) Geological units and Tectonic feature Map of Sana'a basin

3.3 Earthquakes in Yemen and Sana'a region.

Yemen is located in the seismically active zone between the Arabian and African tectonic plates which are pulling apart. The western and southern portions of Yemen around the rifts of the Red Sea and Gulf of Aden represented by volcanic mountains over magmatic champers. These portions

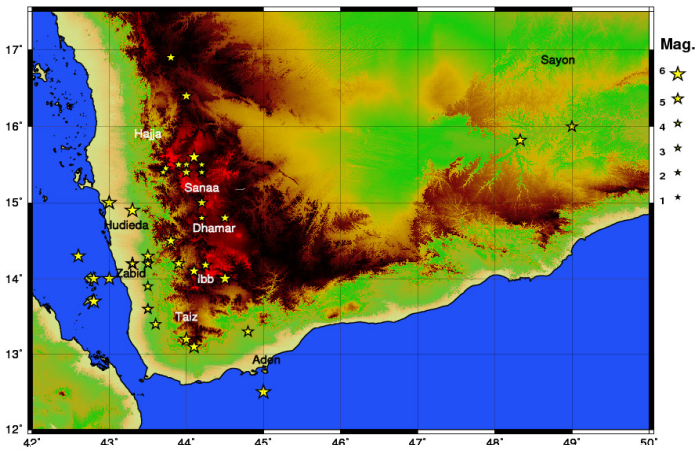

Figure.(4) Historical Earthquakes Map (742-1900)

are the most active seismic zones with moderate to strange level and at risk from earthquakes. Figures.4. and 5. states historical and recent seismicity maps respectively. Although the magnitudes of these events are small but it is felling by peoples living in that areas due to topography and geological condition of Yemen.

On 13 December 1982, a destructive ea of Yemen, causing widespread damag intensity map of Dhamar earthquake. in a densely populated region about 70 injured 1,500 people and damaging mo waves were perceptible as far as Jizan, In particular of Sana'a seismicity , the l by destructive earthquakes in the past

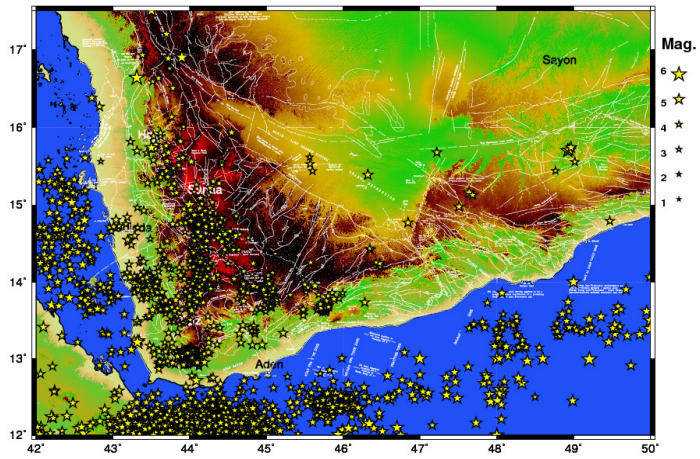

Figure.(5) Recent Earthquakes Map (1900-2007)

periods (742 BC,1644 and 1908) with equivalent magnitudes (M5.0, M5.7 and M6.0) respectively. As well as, it was not far from impacts of the strongest earthquake (Mw6.2) which occurred in Dhamar in 13, Dec.,1982. Further more, many of small earthquakes of magnitude less than 4.2 occurred on the period(1995-2012) highly felt by most of peoples

4. Identification of Building Types at Sana'a City :

4.1 Buildings Spatial Distribution.

The district level residential building data of Sana'a city, obtained from Central Census Organization CCO (2004) includes general information's about population and number of dwellings. It is noticed that the building data base inventory not accurate enough. For example, number of dwellings includes number of apartments and it doesn't contain geographical location and age of each building. Further more, there is no details information on buildings materials type and number of stories for buildings constructed at each district level.

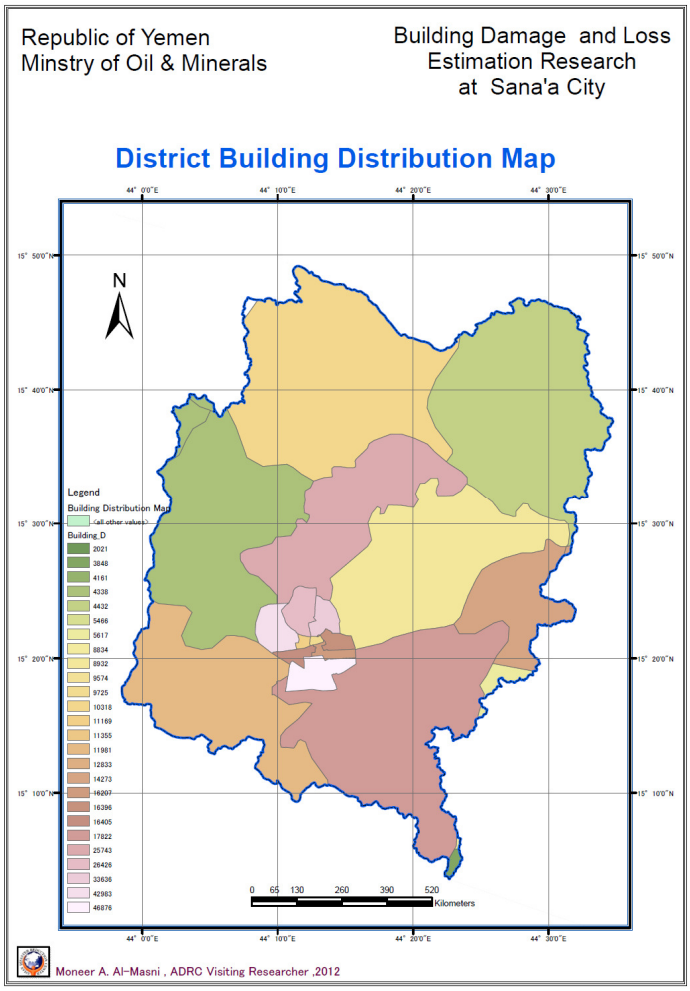

Figure.(6) Distinct Building distribution map

Therefore, for approximate analysis, we assumed uniform building distribution by using the only available information of total percentage, for each building material types and stories numbers at Sana'a basin (Amana Area) .Figure 6. building distribution map at each district level in Sana'a basin.

4.2 Building Material type and Construction Technique :

Seismic performance of a building influences by construction material and technique. Construction technique is largely depending upon the availability of building material

used for building construction and economic conditions of the building owner . The socio-economic conditions of the people defines the type and construction quality of the building and divided building patterns in to three types. Firstly the independent houses which were built for residential purposes and second the group housing like apartments with multiple purpose use .Third industrial, office and commercial building.

Most of the buildings in Sana'a doesn't follow any regulation and are not constructed based on seismic design building code. For example, independent houses or single-family-residences are built by locals who don't involve architects and engineers and it is mostly based on traditional methods . Whereas group housing like apartment complexes etc. for multiple purpose use, industrial offices and commercial building. designed with seismic considerations and it is strong enough to resist lateral forces of minor quakes but not strong enough and don't meet the building standards .

Even though buildings is only planned for few floors in the initial stages , years later, more floors are added to the same building which makes the structure weak and more vulnerable to earthquake hazards. The dominated construction techniques used in Sana' City are load bearing construction and RC framed construction. Table 1. shows the commonly building materials used in construction of load bearing structure and

RC framed structures at Sana'a City. A building constructed of Stone/Blok/Brick in cement mortar will behave much better than constructed of Stone/Blok/Brick in mud mortar.

Table 1. shows the commonly building materials used in construction

Construction Technique	Structural element	Wall material	Type of mortar	Roof material	Floor Material
Load bearing	Stone/Blok/Brick column	Stone/Blok/Brick	Mud, cement	RBC,GI,RCC	RBC,RCC
RC framed	RCC column, beam	Stone/Blok/Brick ,RCC	Cement	RCC	RCC

For building types classification, the buildings with the same material and construction type are grouped into one class. The main classes in Sana'a as explained below:

4.2.1 Un Reinforcement Masonry Structures (URM)

These buildings represents approximately (47 %) of Sana'a building city and constructed of stone , block ,clay or burned brick with cement or mud mortar as shown in Figure.7. It doesn't have any seismic design considerations and therefore, it falls under pre-code category of HAZUS classifications

In Sana'a ,old heritage structures all buildings constructed of burnet bricks and clay and are also vulnerable to earthquake hazards.

Figure.(7) URM Masonry Building (Brick ,stone and clay

4.2..2 Reinforcement Masonry Structures (RM)

These buildings represents approximately (53%) of buildings in Sana'a city . Based on HAZUS technical Manual prepared by FEMA (2011) the structures concrete frame buildings with unreinforced masonry infill walls is defined as RM building class as shown in Figure.8 and 9. The frames can be located almost anywhere in the building. Usually the columns have their strong directions oriented so that some columns act primarily in one direction while the others act in the other directions. In these buildings, the shear strength of the columns, after

Figure.(8) RM structure , RC filled with stone

cracking of the infill, may limit the semi-ductile behavior of the system. In earthquakes these building fail and lead to partial or fall collapse because of brittle failure as these are only designed with ductile properties. Buildings with some level of seismic design were considered but they do not match with the suitable level of building codes and therefore, were considered as low-code category of HAZUS classifications

Figure.(9) RM structure , RC filled with stone

4..3 Building Seismic Design level :

To resists the internal forces caused by earthquakes, it is helpful if the materials perform well both in compression and in tension. Materials, which perform well only in compression, are often reinforced by other materials with good tensile strength qualities..

Unfortunately, no building codes are available for Yemen and the default was to adopt the codes used in the USA (with the necessary modifications). As well as, impossible of development the empirical curves for Yemenis building types, because of absent of analytical functions and due to lack of sufficient damage data in previous earthquakes

Therefore, this research is used the default fragility and capacity parameters that given in HAZUS building types as alternative case following HAZUS methodology.

with consideration to procedures of Prasad et al.(2009) study for identifying and classify the building types due to similarity between Indian and Yemeni's building construction and material types.

Prasad et al.(2009) compared the classified Indian building types to the HAZUS model building types as shows in Table 2, and found out that Indian framed structures have similarity with US buildings and can consider some of it with in low to moderate code of

the HUZUS building types. whereas, the Indian adobe and masonry building types can not compared to any of the fragility curves that are given in default HAZUS building types and it is considered pre-code.

Masonry consisting of Rectangular Units					
9	Burnt clay brick/ rectangular stone in mud mortar	R1, R2	1-2		Not Defined
10		R3, R4	1-2		
11		R5	1-2		
12	Burnt clay brick/ rectangular stone in lime-surkhi mortar	R1, R2	1-2		
13		R3, R4	1-2		
14		R5,R6	1-2		
15	Burnt clay brick/ rectangular stone/ concrete blocks in cement mortar	R1, R2	1-2		
16		R3, R4	1-2		
17		R5,R6	1-2		
18			3+		
19	Burnt clay brick/ rectangular stone/ concrete blocks in cement mortar and provided with seismic bands and vertical reinforcement at corners and jambs	R5,R6	1-2		Not Defined
20			3+		
Framed Structures					
21	RC frame/ shear wall with URM infill's – constructed without any consideration for earthquake forces	R-6	1-3	C3L	Precode
22			4-7	C3M	
23	RC frame/ shear wall with URM infill's - earthquake forces considered in design but detailing of reinforcement and execution not as per earthquake resistant guidelines (Low-Code/Moderate-Code)		1-3	C3L	Precode/Low code
24			4-7	C3M	
25			8+	C3H	
26	RC frame/ shear wall with URM infill's - designed, detailed and executed as per earthquake resistant guidelines (Low-Code/ Moderate-Code/High Code)		1-3	C3L	Precode/Low code/Moderate Code
27			4-7	C3M	
28			8+	C3H	

Table 2. Comparison between classified Indian building types to the HAZUS model Prasad et.al.(2009)

5. Earthquake Building Risk Assessment

Building damage caused by earthquakes contributes to disasters and causes casualties and fires. Earthquake damage to buildings is greatly influenced by the types of buildings. There are various ways to classify buildings, namely by materials, construction type, building age, story or height and usage, etc. It is desirable to adopt the classification based on the factors that closely correlates to observed past damages. However, since detailed building information is not available in many cases, a general classification is often used. We used the following classification categories, adopted based on HAZUS methodology which calculates the building damage in terms of probability of damage of particular model building types for each damage states. The probability of damage is calculated in relationship with given ground motion parameters to evaluate the building performance for a particular seismic event.

The StrucLoss 1.5 Software- developed by Earthquake and Structural Department of Gebze Institute of Technology, Turkey - is used for risk assessment analysis in Sana'a city. The general process of damage estimation from assumed earthquake scenarios is summarized in this section and illustrated by the Figure.10. below.

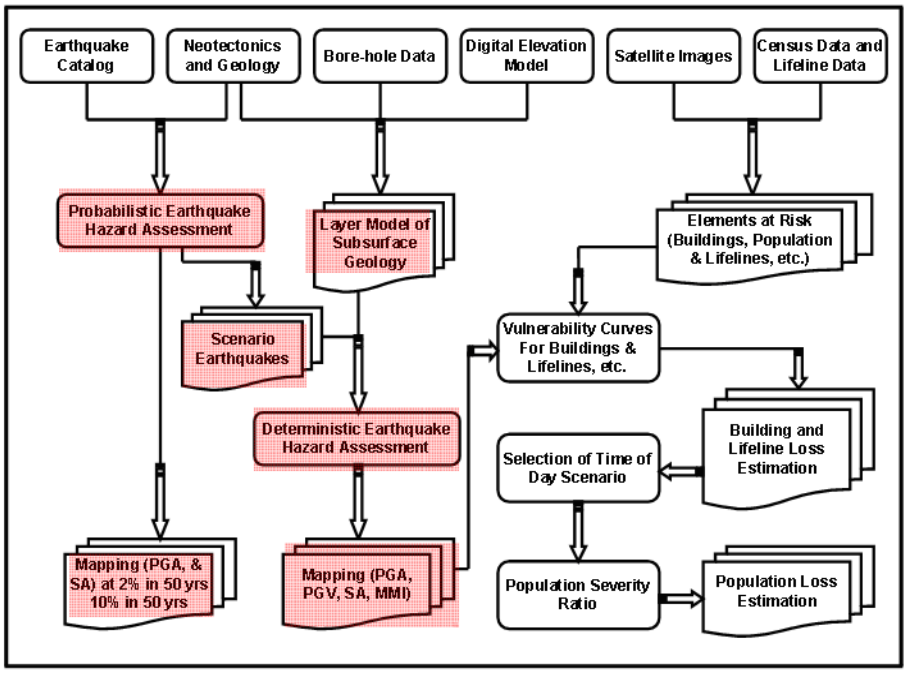

Figure (10) diagram show the methodology used for risk assessment

5.1 Development of Earthquake Scenarios.

The objective of creation earthquake scenario is to describe the results of the damage estimation in a comprehensive and easy to understand manner.

In the present research two synthetic earthquake scenarios were simulated around Sana'a basin as shown in Figure 11. These scenarios seems to be the most important due to their reoccurrence interval for such an event is every hundred to thousand years . As well as, it considers the strongest events locate very close to Sana'a city. More details of these assumed scenarios as mention below:

5.1.1 Assuming Hamdan Earthquake Scenario:

This is the first simulation scenario, called "Hamdan Earthquake Scenario" this event mentioned in historical documents that hit Sana'a and adjacent areas in 1644 with equivalent magnitude to Mw = 6.0 and caused several damages and losses . It was set at the location 15.40N 44.00E and 20km west Sana'a city.

5.1.2 Assuming Dhamar Earthquake Scenario:

The second scenario called "Dhamar Earthquake Scenario" hit Dhamar in 13 Dec.,1982 . It is consider as modern strong earthquake with magnitude Mw6.2, depth 7km and epicenter located at 14.7°N and 44.2°E. and 70km south of Sana'a. This event hit Dhamar and adjacent area caused a lot of damage and earth cracks in Dhamar and Sana'a. The shock waves were perceptible as far as Jizan, Najran and Taiz, all at an average distance of 230 km.

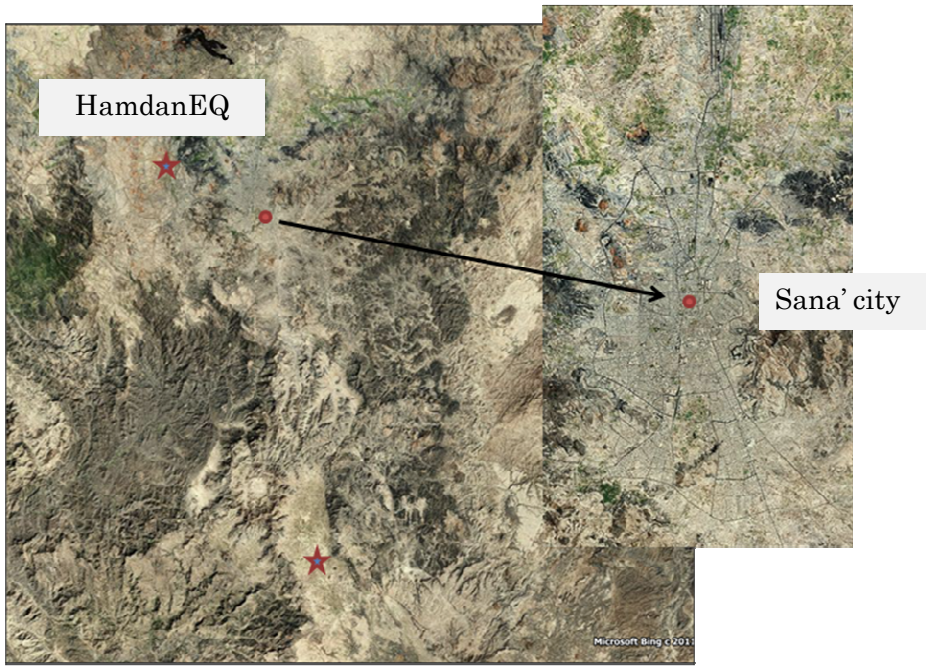

Figure 11 shows the location of earthquakes used for scenario damage assessment

5.2 Deterministic Seismic Hazard Assessment

The geological and seismological information are the basis for appropriate simulation, and these are usually given in broad terms, involving the location, magnitude, rupture length. And attenuation relation. Attenuation models provide the severity of the ground motion in respect to the source magnitude and mechanism, distance to the epicenter and local soil effects.

5.2.1 Soil conditions:

For estimating the local soil effects, the present study used the site geotechnical class-map of Al-Subai et al. (2006) and site effect study using Microtremor array survey (SPAC) by Al-Masni et al.(2008) to estimate average shear wave velocity (Vs30) in quaternary deposits. Whereas, (Vs30) of geological rock units such as Igneous, Metamorphic, Volcanic, and old sedimentary rocks was calculated from the information's of standard typical values of P-wave velocity structure range, Nick, Barton , (2007) and correlated with the Vs30.

Then, geological unites are divided to five classes, from hard rock (A) to soft rock (E) as shown in Fig.(?) according to the classification system recommended by the National Earthquake Hazard Reduction Program (NEHRP) (FEMA, 1997).

5.2.2 Seismic ground motion model :

Deterministic hazard was evaluated using both intensity and ground motion parameters (PGA and SA) based on appropriate attenuation relationships following below. For both cases the median (50-percentile) value obtained from the used attenuation relationships was adopted. The selected ground motion parameters of analysis are the Peak Ground Acceleration (PGA) and the Spectral Acceleration (SA) at periods of 0.2, 0.3 sec and 1.0 sec . A comparison of the attenuation relationships of Ambraseys et al. (1996) and Boore et al. (1997) with New Generation Attenuations (Abrahamson and Silva, 2008, Boore and Atkinson, 2008, Campbell and Bozorgnia, 2008, Chiou and Youngs, 2008) are plotted in Figure 12. For near source conditions, Ambraseys et al. (1996) attenuation highly

overestimates the peak ground acceleration. In this study, for earthquake scenario I and II, Boore et al. (1997) and average of Boore et al. (1997) & Ambraseys et al. (1996) is utilized for the calculation of the PGA and SA for the periods: 0.2, 0.3 and T = 1.0 sec

Based on HAZUS99 recommendations peak ground velocity (PGV) has been calculated from SA at T=1.0 using the following formula:

$$PGV = \left(\frac{386.4}{2\lambda} \cdot S_{A1} \right) / 1.65$$

Where S_{A1} is the spectral acceleration in units of g, at T=1.0sec.

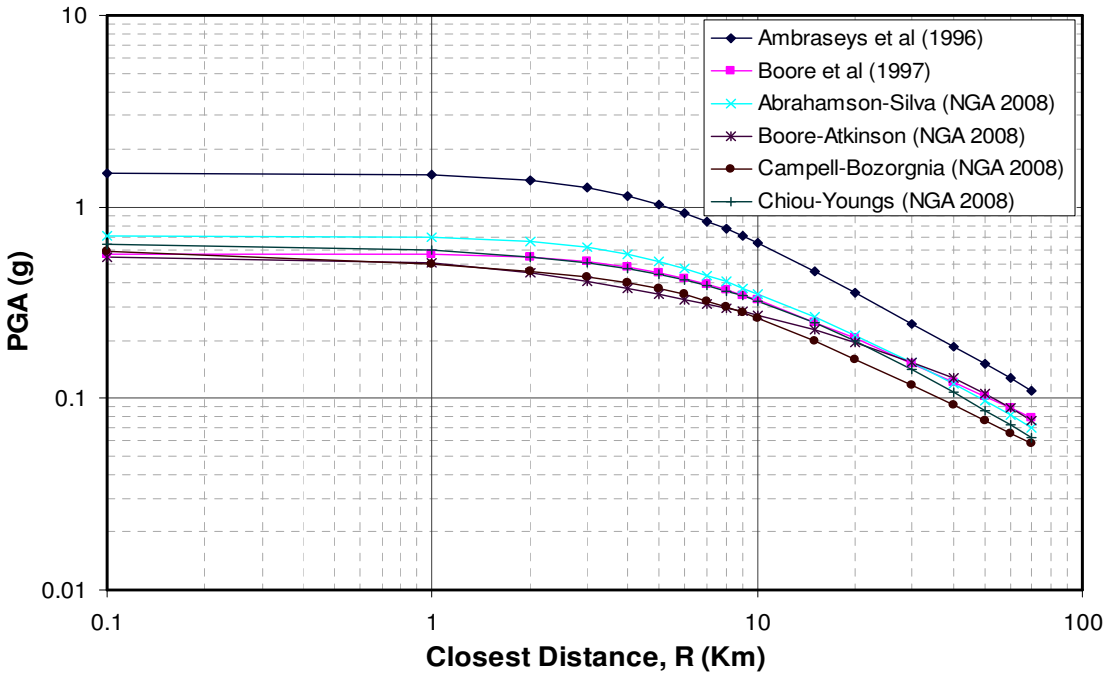

Figure 11: Comparison of PGA Attenuation Relationships for soil type B

5.2.2.1 Intensity Based Deterministic Earthquake Hazard

The empirical relationships between PGA, PGV and Modified Mercalli Intensity (MMI) of Wald et al. (1999) which were developed for the San Andreas Fault area, were investigated for the estimation of the intensity attenuation using the following equations:

$$I_{mm} = 3.66 * \log PGA - 1.66, \text{ for } V \leq I_{mm} \leq VIII$$

$$I_{mm} = 3.47 * \log PGV + 2.35, \text{ for } V \leq I_{mm} \leq IX$$

The average for these equations was favorably comparable with the isoseismal maps of the previous earthquakes (i.e Dhamar,1982). However, comparing these results against PGA-MMI relationships used for Greece, Turkey and Palestine (Bendimerad, 2008 - Personal communication) proved to be significantly conservative for all PGA levels, suggesting that intensities may be under-estimated. Based on local studies, Bendimerad (2003-Unpublished) suggested a PGA-MMI equation for the region:

$$I_{mm} = 1.6 * Ln\ PGA + 0.545 * Mw + 5.78$$

Figure 13. shows a comparison between the results based on equations of Walid et al. (1999) and Bendimerad (2008) for a magnitude of 7.5 against distance. Accordingly, deterministic modeling of the seismic hazard is calculated in terms of the distribution of site-dependent intensities, based on the intensity attenuation of Bendimerad (2003).

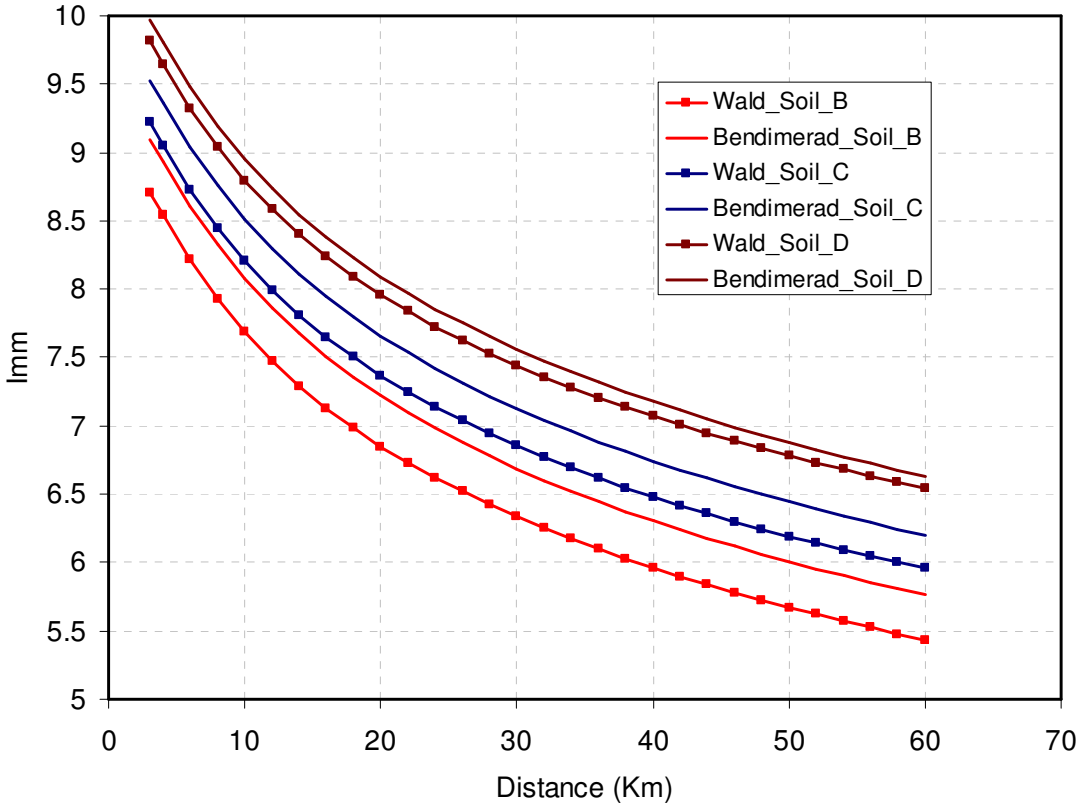

Figure 13: Comparison of the intensity for different soil types using Wald (1990), based on the average of PGA and PGV, and Benimerad (2003) equations.

5.2.2.2. Site Dependent Intensities Spectral Accelerations

Spectral accelerations (SA) for T=0.2, 0.3 and 1.0 sec will be modified according to the 1997 NEHRP Provisions (FEMA, 1997) of site coefficients presented in Tables 3. and 4. These amplified spectral accelerations are later used in the construction of the standard shape of the response spectrum. The standard shape of the response spectrum is taken equal to the so-called "Uniform Hazard Response Spectrum" provided in 1997 NEHRP Provisions (FEMA, 1997). This spectrum, which is employed to assess the demand on structures (for vulnerability analysis), is approximated with the site-specific short-period (S_{ms}) and medium-period (S_m) spectral accelerations as illustrated in Figure 14. S_{ms} and S_m are represented by the calculated SA at T=0.2 sec and T=1.0 sec, respectively. using given formula.

$$Ln((S_A) = b1 + b2(M - 6) + b3(M - 6)2 + b5\,Ln(r) + bvLn\left(\frac{Vs}{VA}\right)$$

Where

$$r = \sqrt{r_{jb}^{2} + h^{2}}$$

And

$$b1 = \begin{cases} b1_{ss} & \text{For strike-Slip earthquakes} \\ b1_{Rv} & \text{For reverse Slip earthquakes} \\ b1_{all} & \text{If mechanism not specified} \end{cases}$$

S_A is spectral acceleration to be derived

b_1, b_2, b_3, b_5, b_v are constants provided with the equation

M is the magnitude of the earthquake

r_{jb} is the horizontal distance from epicenter

V_s the shear wave velocity of the soil class provided by NEHRP classification

Table 3.: Short period site-correction defined

in the 1994 and 1997 NEHRP Provisions (BSSC, 1995 &1998).

Site Class	Ss≤0.25	Ss=0.50	Ss=0.75	Ss=1.0	Ss≥1.25
A	0.8	0.8	0.8	0.8	0.8
B	1	1	1	1	1
C	1.2	1.2	1.1	1	1
D	1.6	1.4	1.2	1.1	1
E	2.5	1.7	1.2	0.9	-
F	-	-	-	-	-

Table 4: Long period site-correction defined
in the 1994 and 1997 NEHRP Provisions (BSSC, 1995 &1998)

Site Class	S1≤0.1	S1=0.20	S1=0.3	S1=0.4	S1≥0.5
A	0.8	0.8	0.8	0.8	0.8
B	1	1	1	1	1
C	1.7	1.6	*1.5*	1.4	1.3
D	2.4	2.0	1.8	1.6	*1.5*
E	*3.5*	3.2	2.8	2.4	-
F	-	-	-	-	-

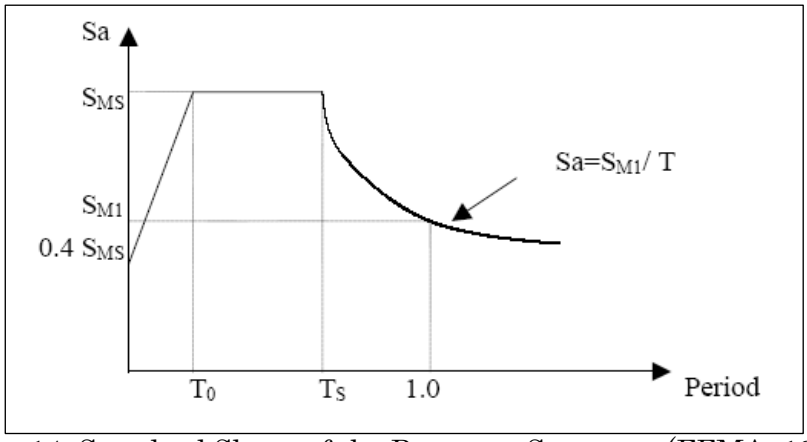

Figure 14. Standard Shape of the Response Spectrum (FEMA, 1997).

5.3 Building Vulnerability Assessment

Earthquake vulnerability of a building is defined as the amount of expected damage induced to it by a particular level of earthquake intensity. Vulnerability is a function of magnitude of an event and the type of elements at risk. The more elements at risk the higher will be the vulnerability.

There are two methods for the analysis of building vulnerability; namely qualitative and quantitative methods. The qualitative method is based upon the statistical evaluation of past earthquake damage. This method is suitable for non-engineering buildings that have the same type of building character. The quantitative method is based upon the numerical analysis of the structure. The buildings with the same material and construction type are grouped into one class. The performance of the buildings is predicted based upon design specifications and construction details. Using these curves damage description is provided for each building class in each damage state including: None, Slight, Moderate, Extensive and Complete (Figure 15 and

Figure エラー! 指定したスタイルは使われていません。).

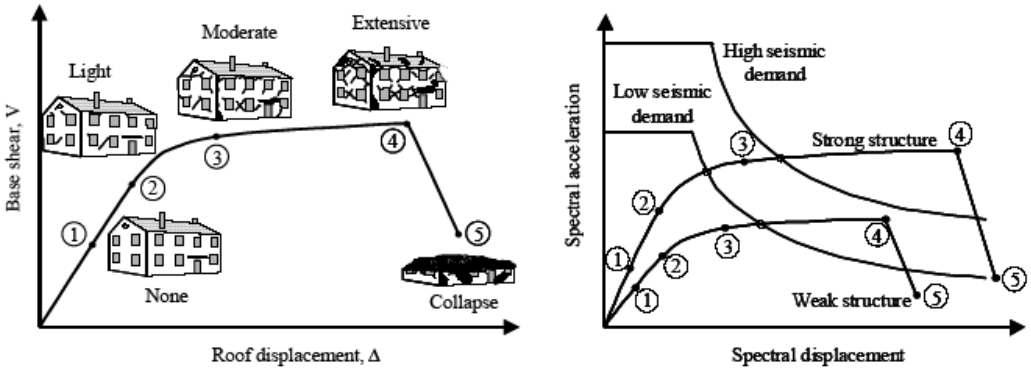

(a) Damage states shown on V-Δ curve (b) Damage levels based on seismic demand

Figure 15: Structural vulnerability and damage states for various levels of seismic demand.

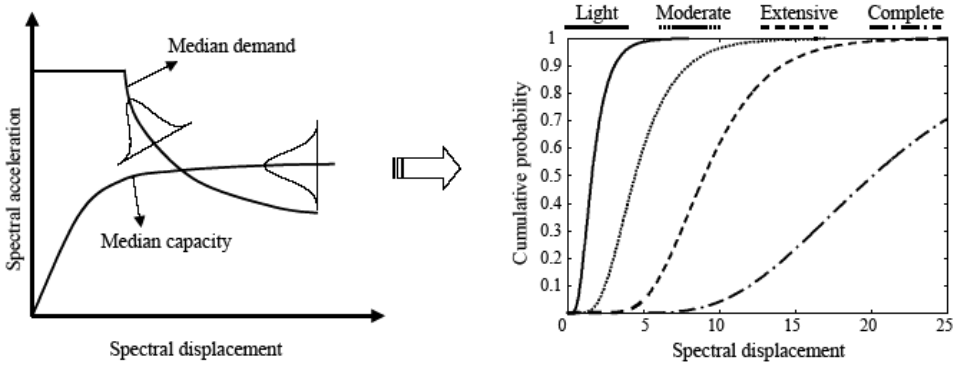

(a) Uncertainties in seismic capacity and demand (b) fragility curves for various damage states

Figure エラー! 指定したスタイルは使われていません。: Uncertainties in seismic performance and use of fragility curves.

Construction of the fragility or damage curves is the key element in estimating the probability of various damage states in buildings or building components as a function of the magnitude of a seismic event..

5.3.1 Building Vulnerability Definitions

The European Macroseismic Scale (Grünthal, 1998), differentiates the structural vulnerabilities into six classes (A to F). Reinforced Concrete buildings with low levels of earthquake resistant design are assigned an average vulnerability class of C. Due to deficiencies in design, concrete quality, lack of direct engineering supervision, and construction practices, the bulk of the reinforced concrete building stock in Sana`a may be considered in this vulnerability class.

Table エラー! 指定したスタイルは使われていません。. and Figure 4.3 illustrate the different damage grades of reinforced concrete buildings (Figure 15). Similarly, Coburn and Spence (1992) incorporated these classes into the definition of the state of damage of masonry buildings (Table 6).

Table エラー! 指定したスタイルは使われていません。: Damage grades definition (Grünthal, 1998)

Grade	Description
D1	Negligible to slight damage (No Structural Damage (SD), Slight

	Non-Structural Damage (NSD))
D2	Moderate damage (Slight SD, Moderate NSD)
D3	Substantial to heavy damage (Moderate SD, Heavy NSD)
D4	Very heavy damage (Heavy SD, very heavy NSD)
D5	Total Destruction.

Table 6: Damage grades of reinforced concrete buildings (Grünthal, 1998)

Damage Grade	Masonry Buildings	RC Buildings
D1-Slight	Hairline cracks	Panels cracked (Non-structural)
D2-Moderate	Cracks 0.5-2cm	Structural Cracks <1cm
D3-Heavy	Cracks >2cm or wall material dislodged	Heavy damage to structural members, loss of concrete
D4-Partial Destruction	Complete collapse of individual wall or roof support	Complete collapse of individual structural member or major deflection of structure
D5-Collapse	-	Failure of structural members to allow fall of slabs.

Moreover, Grünthal (1998) tied the grade of damage of reinforced concrete buildings with low levels of earthquake resistant design with the definitions of earthquake intensities Table 7.

Table 7: Definitions of earthquake intensities tied to the grade of damage of reinforced concrete buildings (Grünthal, 1998).

Intensity	Damage Description*
Intensity VI	A few buildings of vulnerability class C sustain Damage of grade 1.
Intensity VII	A few buildings of vulnerability class C sustain damage of grade 2.
Intensity VIII	Many buildings of vulnerability class C suffer damage of grade 2; a few of grade 3.
Intensity IX	Many buildings of vulnerability class C suffer damage of grade 3; a few of grade 4.
Intensity X	Many buildings of vulnerability class C suffer damage of grade 4; a few of grade 5.

*Where “Few” describes less than 20% and “Many” describes between 20% and 60%.

For the general indication of vulnerability in different earthquake intensity zones; Coburn (1987) defined the following damage percentages of various building material

of heavy damage to collapse classes (Table 8).

Table 8: Vulnerability of building stock in different hazard zones (Percent Damage).

Io(MSK)	Percent Damage for Building Type					
	Poor Masonry		Good Masonry		RC	
	>=D3	D5	>=D3	D5	>=D3	D5
>IX	90%	50%	60%	5%	50%	1%
VIII	75%	5%	50%	1%	5%	-
VII	50%	1%	5%	-	1%	-

It can be said that existing vulnerability functions vary in there response according to the building structure and associated building materials.

5.3.2 Building inventory

For an effective estimation of damage to buildings, a building classification is necessary. Buildings may be classified according to various parameters. For example, building may be classified according to their material types, usage, age, structural types and local building codes, etc. Development of realistic fragility curves for the building stock and lifelines in Sana'a building inventory is essential for seismic risk analysis such as damage, social and economic losses. In HAZUS (FEMA, 2003; FEMA, 2006a, b), the building inventory classification system is utilized to group buildings with similar characteristics into a set of pre-defined building classes, commensurate with the relevant vulnerability relationship classes. For a general building stock, the Structural (e.g., height); Nonstructural elements; and Occupancy (e.g., residential, commercial, and governmental) are the parameters that affect and characterize the damage and loss.

Overall, the HAZUS presents four main building types: wood, masonry, concrete and

steel, and these can be further subdivided into 36 classes according to the building height and seismic design level (for more details see HAZUS Technical Manual, chapter 3).The HAZUS building damage functions, which are formulated as fragility curves, describe the probability of reaching or exceeding discrete states of damage for the structure and nonstructural systems. The states of the damage are: None, Slight, Moderate, Extensive and Complete. Descriptions of these damage states are found in the HAZUS Technical Manual (FEMA, 2003; FEMA, 2006a, b).

Since there are no damage functions available for Yemen, the present study used the default capacity and fragility parameters functions given by the HAZUS for all types of loss. The building stock used in this research consists of about 260,000 buildings/Dwellings based on Census tract 2004 . The stock was classified in to five groups according to types of construction materials, year of built, the number of stories and the seismic design level. As well as, the total buildings number for each class has been computed. Figure 17. shows the statistical classification of the buildings based on constriction materials and number of stories in term of Low- rise , Mid- rise and High -rise buildings.

The simulations of the loss estimation were thus based on these groups, ranging from the worst-case scenario that included the URM-Pre code, up to the RM –Low code. These two building types set the maximal and minimal loss estimations, suggesting the actual damage should be somewhere in between. In order to improve and perform a better and more accurate estimation of the losses, it is essential to develop the local damping, capacity and fragility curves typical for the Yemeni building types. Following an explanation procedure for modeling the buildings based on type, height and age (Seismic Design Consideration).

Construction Type (I)

1. Reinforcement concrete building filled with masonry block.
2. Reinforcement concrete building filled with masonry stone..

3. Masonry (Stone/concrete Block) buildings
4. Masonry (Bricks) buildings
5. Masonry (Clay) buildings

Number of stories (J)

1. Low -rise (1-3 stories)
2. Mid -rise (4-6 stories)
3. High-rise (more than 6 stories)

Construction date (K)

1. Construction year: Pre-1982
2. Construction year: Post-1982

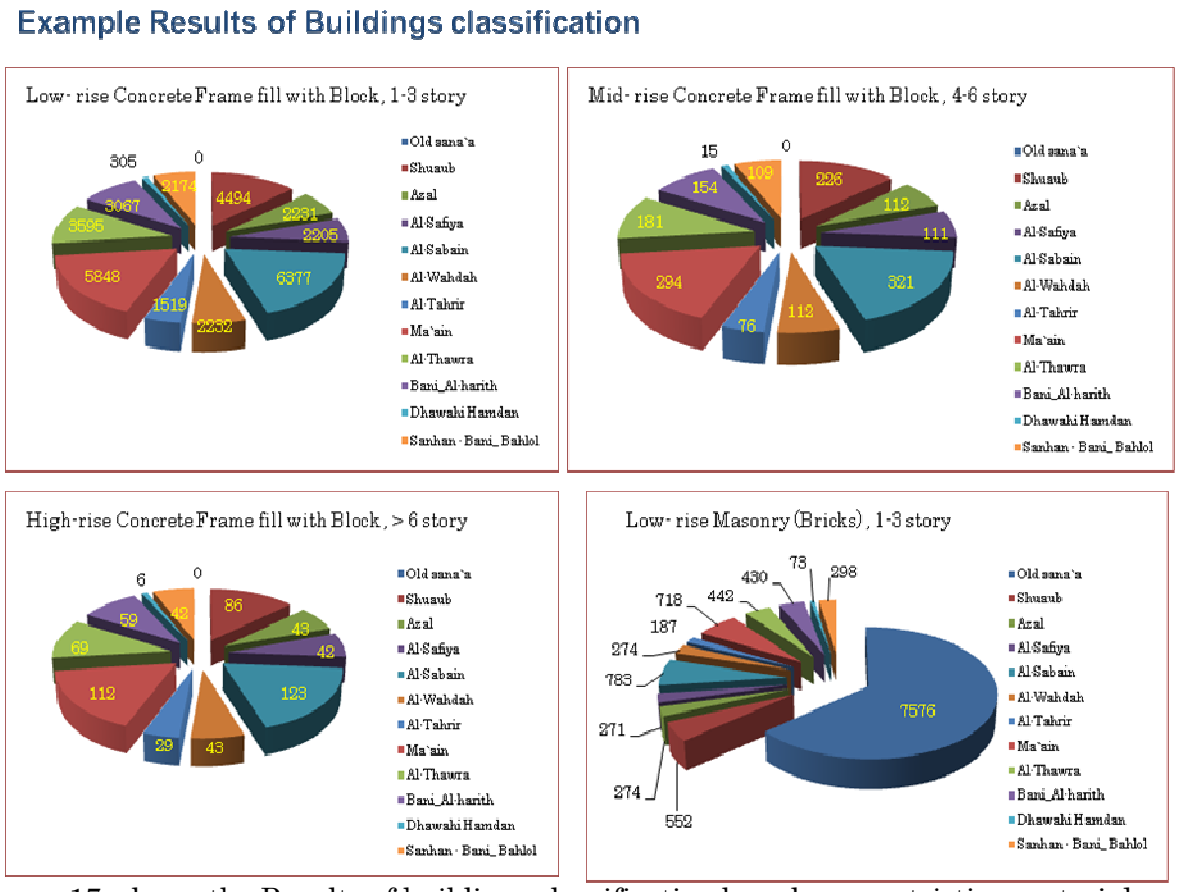

Figure 17. shows the Results of buildings classification based on constriction materials and number of stories in term of Low- rise , Mid- rise and High -rise buildings

5.3.3 Building Damage Analysis

Buildings respond to ground shaking in earthquakes. As buildings are tied to the ground with foundations, the free end i.e., roof shakes more than the ground. There is

always some inbuilt strength to resist this shaking. But when it reaches it maximum levels, it tends to reach its upper limit and finally collapses. Till a limit, in built strength of the building resist the shake and allow the building remains stiff and stand straight , this is called yield capacity point. When building reaches it is yield capacity it starts to shake to a limit and at a stage the building loses it complete strength and can no longer resist the force of shaking and structural system completely fails. That point before losing all strength to shake is called ultimate capacity point. The capacity curve is generally derived from two points.

Kircher et al. (1997) describes capacity and fragility curves functions which are used by HAZUS methodology for estimating damage from ground shaking caused by earthquakes. Capacity curves define the non-linear behavior of buildings which are described by the yield and ultimate strength and on the other hand the probability level of damage to the buildings at given ground shaking level is predicted by the fragility curve.

In this study building damage analysis calculated based on spectral displacement as following steps:

5.3.3.1 Spectral Displacement Based Fragility Curves

In spectral displacement-based fragility curves, the horizontal axis represents the spectral displacement demand and vertical axis refers to the cumulative probability of structural damage reaching or exceeding the threshold of a given damage state. Therefore, it is required to determine the spectral displacement demand of a given structure for a given earthquake action.

5.3.3.2 Analytical Basis of Fragility Curves

The analytical expression of each fragility curve is based on the assumption that earthquake damage distribution can be represented by a lognormal distribution function (FEMA 1999, Kircher et al. 1997):

$$P\,[D \geq ds \mid S_{di}] = \Phi\,[(1/\beta_{ds})\,\ln\,(S_{di}/S_{d,ds})]$$(エラー! 指定したスタイルは使われていません。.1)

where D refers to the damage, S_{di} is the inelastic spectral displacement demand, $S_{d,ds}$ represents the median value of spectral displacement corresponding to the threshold of the damage state reached – ds (slight, moderate, extensive or complete), β_{ds} is the standard deviation of the natural logarithm of the spectral displacement corresponding to the damage state concerned. Φ refers to cumulative standard normal distribution function. Median spectral displacement values corresponding to each damage state, $S_{d,ds}$, are estimated in terms of story drift ratios specified for each building type. On the other hand, the standard deviation β_{ds} is empirically estimated to cover the uncertainties associated with the definition of the damage level concerned, the building load capacity and the earthquake ground motion specified.

5.3.3.3 Analytical Basis of Structural Capacity

The use of spectral displacement-based fragility curves require the spectral displacement demand of a given structure be determined for a given earthquake action. In HAZUS damage estimation methodology (FEMA 1999), the spectral displacement demand for a given structural type is essentially estimated on the basis of Capacity Spectrum Method (ATC-40, 1996). In this method, inelastic structural capacity of the structure is represented by the so-called "capacity spectrum" (capacity diagram) plotted in terms of spectral acceleration versus spectral displacement.

The capacity diagram of a given structure can be readily estimated through its "yield spectral acceleration", S_{ay}, which is defined as (ATC-40, 1996):

$$S_{ay} = \frac{V_y}{M_{x1}} \qquad (5.2)$$

where V_y represents the base shear capacity at yield and M_{X1} refers to the participating modal mass effective in the first mode of vibration. The latter is defined as:

$$M_{x1} = \frac{W}{g}\alpha_1$$ (エラー! 指定したスタイルは使われていません。

5.3)

in which W represents the total seismic weight of the structure, g is acceleration of gravity and α_1 refers to participating mass ratio.

On the other hand the base shear capacity at yield can be estimated as:

$$\frac{V_y}{W} = C_s\ \gamma\ \lambda$$ (エラー! 指定したスタイルは使われていませ

ん。.4)

where C_s is the approximate value of the estimated design lateral strength factor assumed to be valid for the date of construction (this factor is not necessarily related to the seismic coefficient defined in the codes), γ and λ are the approximate "over-strength factors" estimated according to the date of design/construction. The factor γ represents the ratio of the yield strength to the design strength whereas factor λ is defined as the ratio of the ultimate strength to the yield strength. Building capacities are based on best-estimate approximate factors supported by engineering judgment, without any analysis performed.

Thus, from Eqs 4.4, 4.5 and 4.6 the yield spectral acceleration is obtained as

$$S_{ay} = C_s\ \gamma\ \lambda\ \frac{g}{\alpha_1}$$ (エラー! 指定したスタイルは使われていませ

ん。.5)

A typical capacity diagram is shown in Figure 18, which is idealized to represent an elastic-perfectly plastic behavior. The slope of the initial line corresponds to the square of the natural frequency, which is related to the natural period as $\omega = 2\pi / T$.

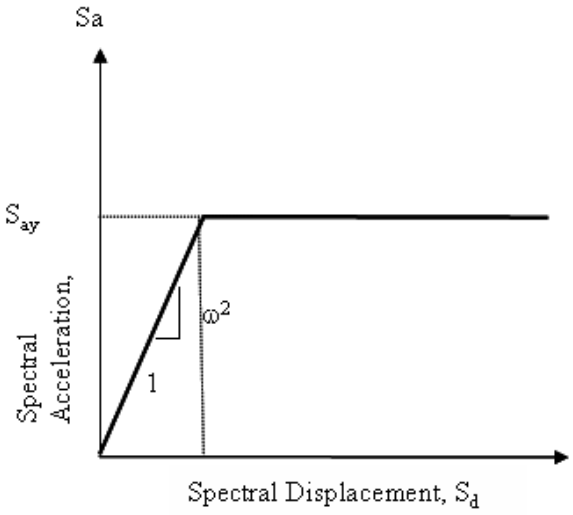

Figure 18. Typical capacity diagram

5.3.3.4 Estimation of Structural Capacity and Fragility Curves

This study adopts the spectral displacement procedure explained above and the risk assessment analyses for buildings are performed using StrucLoss Software. The algorithms and the methodology used in the software are given in Appendix A. Table (8) shows the initial starting values of capacity and fragility curves parameters for different building classes were adopted from HAZUS-MH (2003).

Sana_fragility Browser

BTYPE	MEAN1	BETA1	MEAN2	BEATA2	MEAN3	BEATA3	MEAN4	BEATA4	MEAN5	BEATA5
111	0.54	1.09	0.54	1.09	1.08	1.07	2.7	1.08	6.3	0.91
112	0.54	1.09	0.54	1.09	1.08	1.07	2.7	1.08	6.3	0.91
121	0.9	0.85	0.9	0.85	1.8	0.83	4.5	0.79	10.5	0.98
122	0.9	0.85	0.9	0.85	1.8	0.83	4.5	0.79	10.5	0.98
131	1.3	0.71	1.3	0.71	2.59	0.74	6.48	0.9	15.12	0.97
132	1.3	0.71	1.3	0.71	2.59	0.74	6.48	0.9	15.12	0.97
211	0.54	1.09	0.54	1.09	1.08	1.07	2.7	1.08	6.3	0.91
212	0.54	1.09	0.54	1.09	1.08	1.07	2.7	1.08	6.3	0.91
221	0.9	0.85	0.9	0.85	1.8	0.83	4.5	0.79	10.59	0.98
222	0.9	0.85	0.9	0.85	1.8	0.83	4.5	0.79	10.59	0.98
231	1.3	0.71	1.3	0.71	2.59	0.74	6.48	0.9	15.12	0.97
232	1.3	0.71	1.3	0.71	2.59	0.74	6.48	0.9	15.12	0.97
311	0.32	1.15	0.32	1.15	0.65	1.19	1.62	1.2	3.78	1.18
312	0.32	1.15	0.32	1.15	0.65	1.19	1.62	1.2	3.78	1.18
321	0.5	0.99	0.5	0.99	1.01	0.97	2.52	0.9	5.88	0.88
322	0.5	0.99	0.5	0.99	1.01	0.97	2.52	0.9	5.88	0.88
411	0.41	0.99	0.41	0.99	0.81	1.05	2.03	1.1	4.73	1.08
412	0.41	0.99	0.44	0.99	0.81	1.05	2.03	1.1	4.73	1.08
421	0.63	0.91	0.63	0.91	1.26	0.92	3.15	0.87	7.35	0.91
422	0.63	0.91	0.63	0.91	1.26	0.92	3.15	0.87	7.35	0.91
511	0.32	1.15	0.32	1.15	0.65	1.19	1.62	1.2	3.78	1.18

Sana_Capacity Browser

BTYPE	H	T	ALFA1	ALFA2	GAMA	LAMBDA	CS	C2	KAPPA	SAY
112	6	0.3	0.75	0.75	1.5	2	0.1	1.1	0.4	176
122	15	0.56	0.751	0.75	1.25	2	0.1	1.1	0.4	176
132	24	0.7	0.75	0.6	1.1	2	0.075	1.1	0.4	176
212	6	0.3	0.75	0.75	1.5	2.25	0.05	1.1	0.3	176
222	15	0.56	0.75	0.75	1.25	2.25	0.05	1.1	0.3	176
232	24	0.7	0.751	0.6	1.1	2.25	0.038	1.1	0.3	176
312	6	0.3	0.75	0.75	1.5	2.25	0.05	1.1	0.3	157
322	12	0.4	0.75	0.75	1.25	2.25	0.05	1.1	0.3	157
332	18	0.6	0.75	0.6	1.1	2.25	0.038	1.1	0.3	157
411	6	0.3	0.75	0.75	1.5	2	0.067	1.1	0.3	157
412	6	0.3	0.75	0.75	1.5	2	0.067	1.1	0.3	157
421	15	0.56	0.75	0.75	1.25	2	0.067	1.1	0.3	157
422	15	0.56	0.75	0.75	1.25	2	0.067	1.1	0.3	157
431	24	0.7	0.75	0.75	1.5	2	0.067	1.1	0.3	157
432	24	0.7	0.75	0.75	1.5	2	0.067	1.1	0.3	157
511	6	0.25	0.75	0.75	1.25	2	0.067	1.1	0.3	157
512	6	0.25	0.75	0.75	1.25	2	0.067	1.1	0.3	157

Table 8: Left table show , Building fragility parameters and right table Building capacity parameters

5.3.3.5 Estimation of Spectral Displacement Demand

In the Capacity Spectrum Method (ATC-40, 1996), the spectral displacement demand is obtained through the intersection of the capacity spectrum with the so-called "demand spectrum". The concept of demand spectrum rests on the idea of reducing the elastic acceleration spectrum with an equivalent viscous damping of a linear single-degree-of-freedom (SDOF) system represented by its secant stiffness. There has been a debate since the inception of the method on whether the empirically defined spectrum reduction factors are representative of the inelastic behavior of the equivalent SDOF system. In fact, Chopra and Goel (1999) reported that the Capacity Spectrum Method based the approximate demand spectrum generally overestimates the response by a significant margin. Similar findings are also reported in ATC-55, 2001. The Demand Spectrum is generated by the Equation given by Boore et al. (1997) given below.

$$Ln((S_A) = b1 + b2(M - 6) + b3(M - 6)2 + b5\,Ln(r) + bvLn(\frac{Vs}{VA})$$ (エラー! 指定したスタイルは使われていません。.8)

then from the equation spectral acceleration S_A is derived. Then *SD* is calculated from the equation given below:

$$SD = 9.8 * S_A * T^2$$ (エラー! 指定したスタイルは使われていません。.9)

S_A is the spectral Acceleration calculated from the first equation

T is the time period in seconds as given in the constants provided with the equation

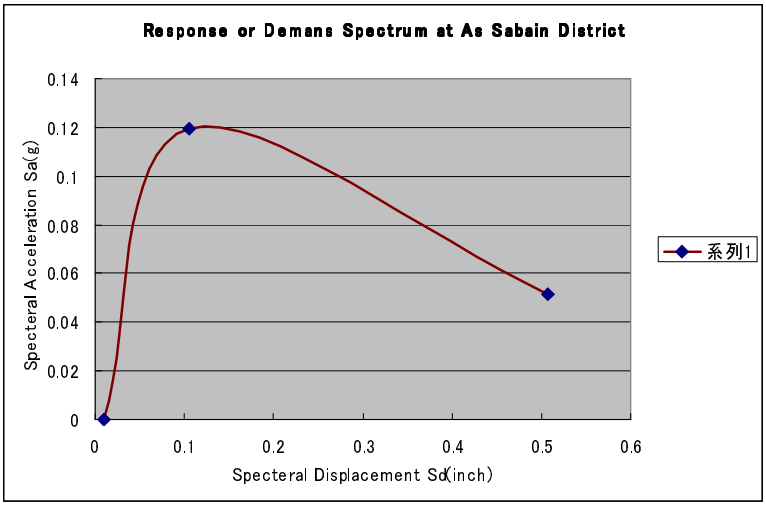

Figure 19 : show response or Demand spectra at Sana'a(Assabain) area

5.3.3.6 Damage probability of all five model building types

The damage probabilities of all five model building types were calculated by method explained above. The damage probability matrix was thus derived for all model-building types for all damage states by using damage algorithm described in Appendix A. Table 9. provides an example of discrete damage probabilities derived from cumulative probabilities given in the example Figure 20.

The damage probability represent the performance of five model building type for a low seismic design code and pre- seismic design code.

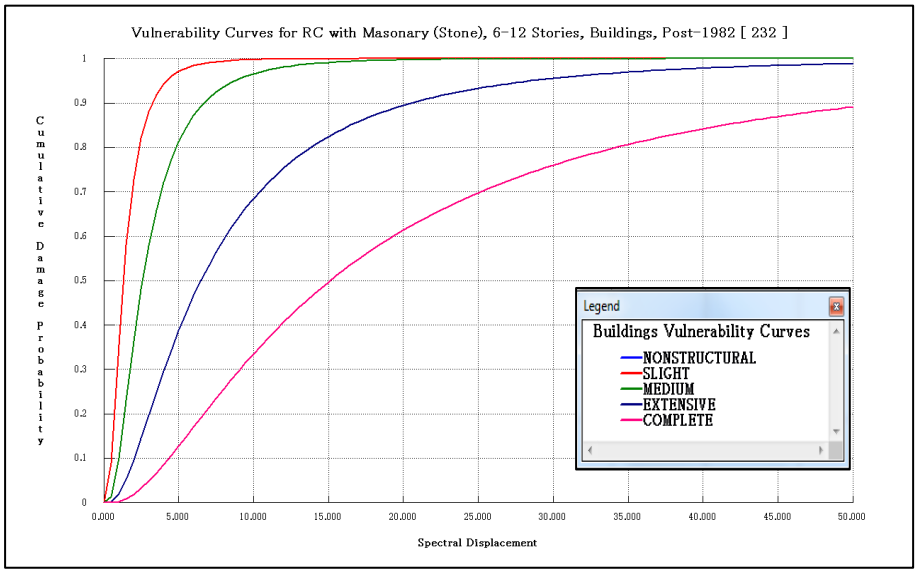

Figure 20 show an example of vulnerability curve of RC type high-rise buildings

GRID_ID	S1	SS	ND232N	ND232I	ND232S	ND232M	ND232E	ND232C	ND232T
1301.0	0.046	0.106	0.0	0.0	0.0	0.0	0.0	0.0	0.0
1302.0	0.044	0.100	165.9	0.0	46.4	11.8	2.3	0.3	226.7
1303.0	0.047	0.108	78.5	0.0	25.4	7.0	1.4	0.2	112.5
1304.0	0.049	0.113	75.2	0.0	26.5	7.7	1.5	0.2	111.2
1305.0	0.052	0.120	208.9	0.0	81.6	25.2	5.1	0.8	321.6
1306.0	0.047	0.109	78.1	0.0	25.7	7.2	1.4	0.2	112.6
1307.0	0.047	0.107	53.7	0.0	17.2	4.7	0.9	0.1	76.6
1308.0	0.044	0.101	215.1	0.0	60.8	15.6	3.0	0.4	294.9
1309.0	0.043	0.098	134.2	0.0	36.1	9.0	1.7	0.2	181.3
1310.0	0.036	0.081	144.0	0.0	26.2	5.3	1.0	0.1	176.6
2301.0	0.020	0.065	28.4	0.0	1.2	0.1	0.0	0.0	29.8
2302.0	0.011	0.036	30.8	0.0	0.2	0.0	0.0	0.0	31.0
2303.0	0.012	0.037	12.9	0.0	0.1	0.0	0.0	0.0	13.0

Table 9. shows an example of discrete damage probabilities of RM H buildings derived from above Vulnerability cumulative curve

6- Discussion and results of Earthquake Building Risk Assessment

The results of expected damage on buildings calculated by HAZUS method, gave good results at the broad level evaluation. However, the results seem not to be very accurate for fine level risk evaluation. The parameters like building response and damage curves of US based building classes could be one of the major factors of getting these results. The accurate values of Yemini's buildings capacity and damage function should be needed to get the more realistic results of risk evaluation of buildings in study area. The difference in structural properties of RM and URM classes with structural properties of framed and masonry buildings in study area could be one other reason of getting inaccurate results of building damage.

The results of earthquake risk assessment calculated from both scenarios with considering ground conditions of study area in Sana'a city are plotted in term of chart diagram in Figures(21,22.23 and 24). As well as the risk map are shown in Figure 25 for describe the

percent of complete damage at all five model buildings in the area. The graphs indicates the building having structural properties similar to URML model building type is the most vulnerable among all five model building types. Whereas buildings having structural properties similar to RM class is least vulnerable to earthquake damage. On the other hand, the buildings located above soft sediments site have higher damage and more vulnerable to risk comparing to buildings located on hard rock . Figure 26. Shows soil amplification map.

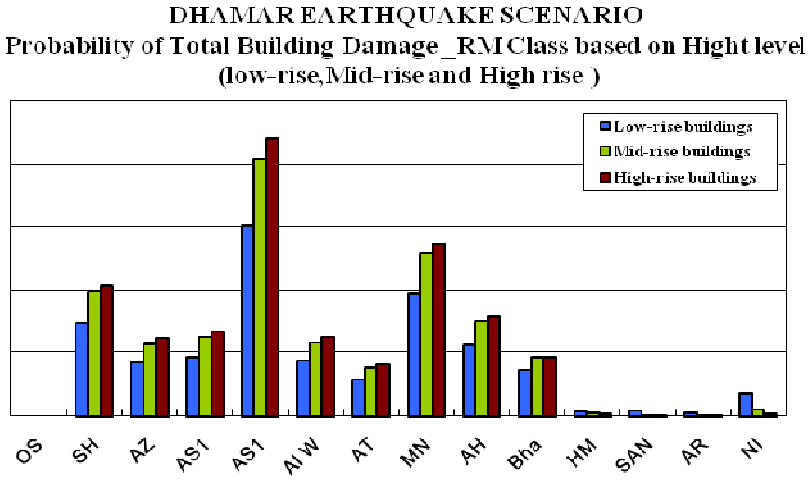

Figure 21 Chart diagram shows Expected damage of RM buildings from Dhamar scenario

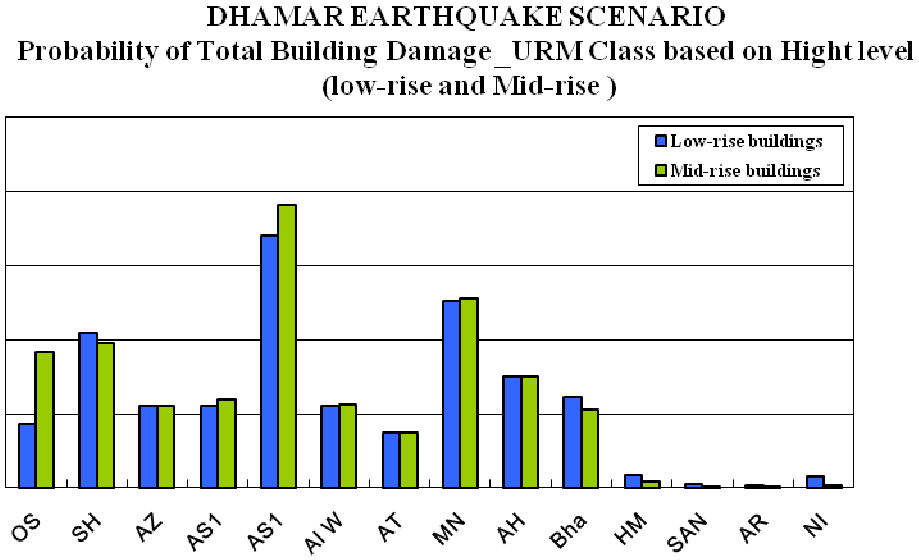

Figure 22 Chart diagram shows Expected damage of URM buildings from Dhamar Scenario

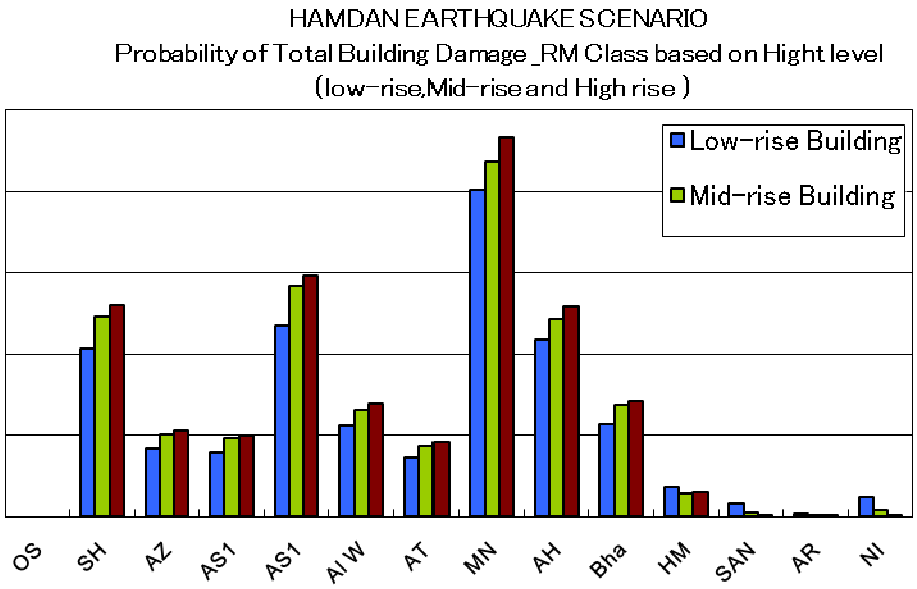

Figure 23 Chart diagram shows Expected damage of RM buildings from Hamdan scenario

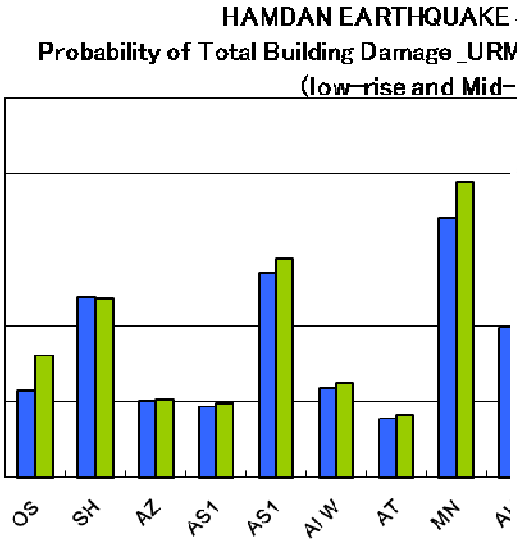

Figure 24 Chart diagram shows Expected damage of RM buildings from Hamdan scenario

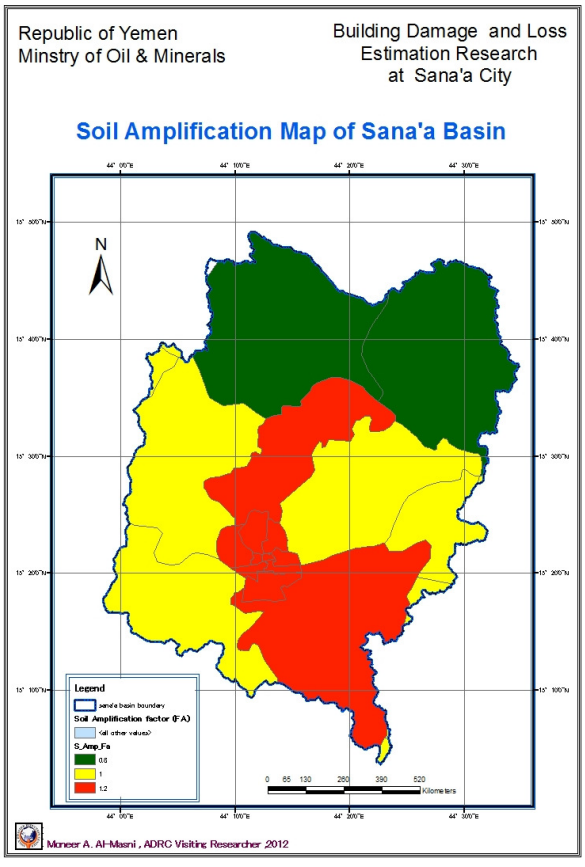

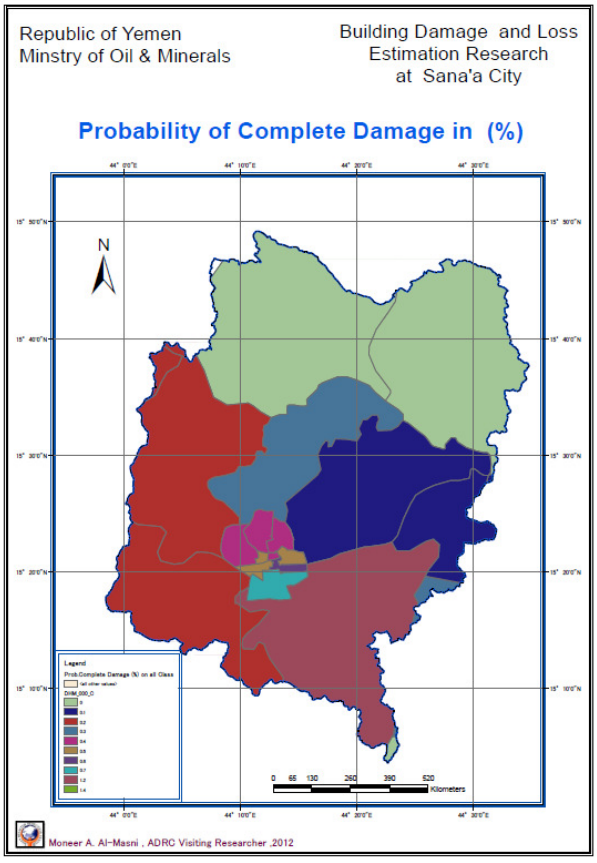

Figure 25 left show Risk Map resulted from Dhamar Earthquake scenario

Figure 26 Soil amplification map at Sana'a basin

Appendix A

StrucLoss 1.5 Software and algorithm

(Updated Version of KoeriLoss 1.0)

StrucLoss 1.5 is an updated version of Koeriloss software. The updated version is developed by Earthquake and Structural Department of Gebze Institute of Technology, Turkey. (http://www.gyte.edu.tr/Dosya/328/Software/StrcuLoss.htm).

Four major developments are included in this version

1. Risk assessment of lifelines including water transmission pipelines, waste water transmission pipelines, gas transmission pipelines, motorways and highways.
2. Integrate the deterministic hazard into the software for widely used attenuation relationships computation is integrated.
3. Line by Line analyses procedure to replace the Grid by Grid procedure. Each line contains a part of the Grid that included in the block. This procedure provides easy and correct way to aggregate the different loss results to Block and Districts.
4. Provide Intensity based outputs of the results for each damage states of each building types. Calibration and testing the capacity curve and fragility curve parameters can be done more accurately and in fast way.
5. Initial input parameters file is included to allow the user to change the default analyses parameters of the software

KoeriLoss 1.0 is developed by the Earthquake Engineering Department of Bogazici University, Kandilli Observatory and Earthquake Research Institute (KOERI). The software applies a loss estimation methodology developed by KOERI to perform analyses for estimating potential losses from earthquakes. KoeriLoss Version 1.0 in its current form is capable to perform building damage estimation analysis using both intensity and spectral displacement based methodology. It is also able to estimate the direct economic losses and casualties related to building damages.

StrucLoss 1.5 is user-friendly software that operates through Geo-cells systems. Geo-cells

(Grids) facilitate the manipulation of data on building stock, population and, earthquake hazards. The software is developed using the MapBasic language and runs efficiently under MapInfo software. Therefore, the software is fully integrated with MapInfo and capable to utilize the powerful features in displaying, querying, manipulating and mapping inventory databases. StrucLoss provides a great flexibility in displaying the outputs. Tables of building damages, social and economic losses can be easily mapped and displayed on the screen, printed or pasted into electronic documents.

Methodology and Algorithm

StrucLoss Estimation Methodology is the basis for the algorithm used to develop the software. General algorithms for spectral displacement based loss estimation are shown in Figure E1.

Classification of Building Data

Classification systems are essential to ensure a uniform interpretation of data and results. Building specifications used in the methodology have been developed to provide the ability to differentiate between buildings with substantially different damage and loss characteristics. The building inventory stocks can be classified using three categories:

-Structural systems category (I)

Example: I = 1 : RC frame building

I = 2 : Shear wall building

I = 3 : Masonry building

- Number of building stories category (J)

Example: J = 1 : 1 – 3 stories (including basement)

J = 2 : 4 – 6 stories (including basement)

J = 3 : > 6 stories (including basement)

- Construction Year category (K)

Example: K = 1 : Construction year: pre-1980 (included)

Example: **K = 2** : Construction year: post-1980

Therefore any building type can be specified as I-J-K where I, J, and K refer to the structural system, number of stories and construction year of the building respectively. To specify a group of building type, wildcards can be used. If 0 is specified as I, J and/or K, all the building types of that group will be considered. The building classification system is discussed thoroughly in section 3.1.

Classification of Structural Damage

The structural damage of the buildings are classified in four groups:

- (1) Slight damage
- (2) Moderate damage
- (3) Extensive damage
- (4) Complete damage

Classification of Casualties

Casualties are classified in four categories of severity:

- Severity 1
- Severity 2
- Severity 3
- Severity 4

Output of the Analysis

The software deterministic hazard part provides the ground motion parameters (PGA, PGV, Intensity and Spectral Accelerations S0.2, S0.3, S1). The loss estimation part provide building damage loss, economic loss and the number of casualties in terms of Geo-cells, sub-districts (Blocks) and districts as MapInfo Output tables.

Lifeline

The lifeline loss assessment estimations are based on methodologies proposed by ATC-25,

HAZUS 2002, ALA 2001 and Japan waterworks associations.

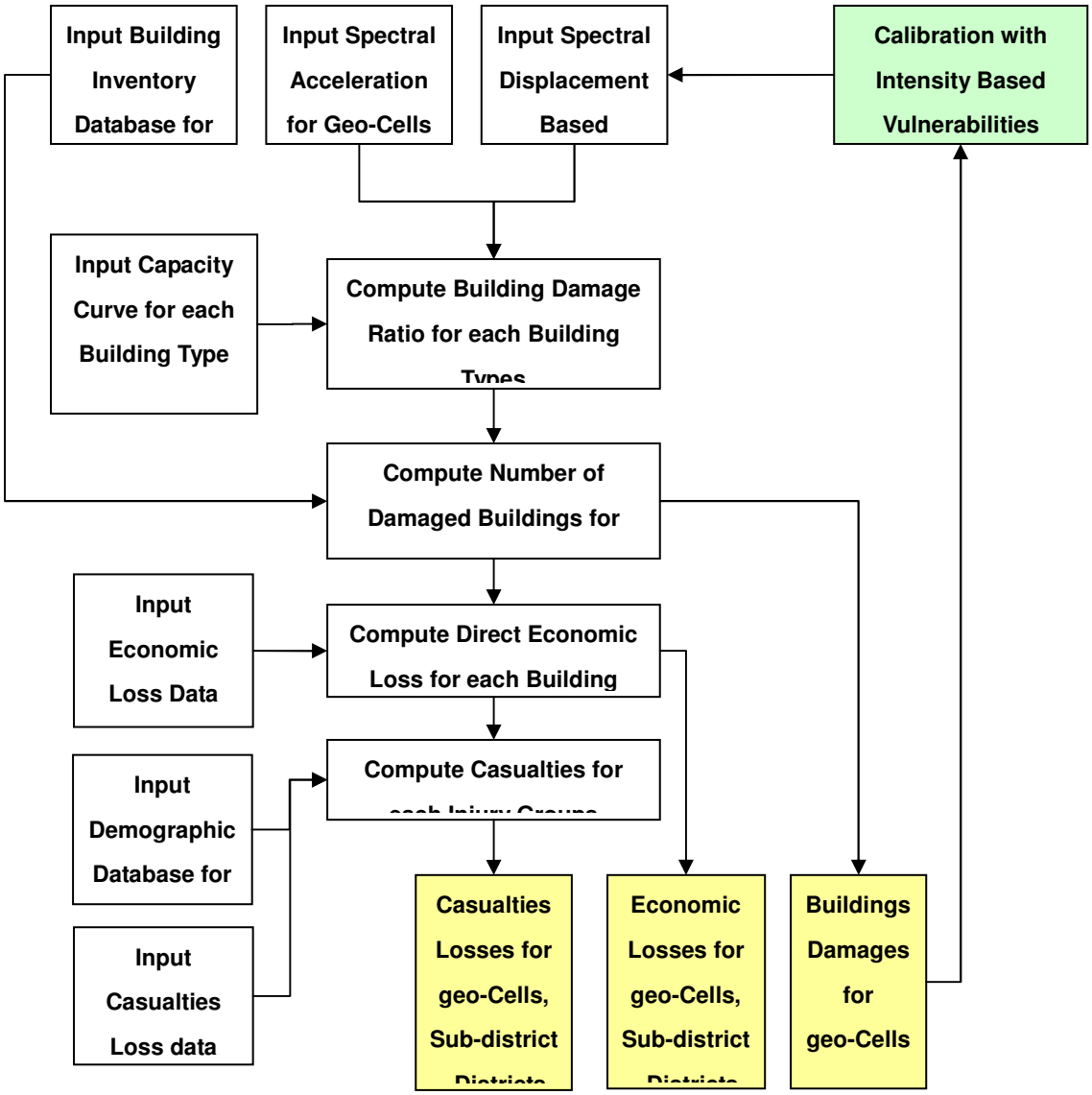

Figure E1: General Algorithm of StrucLoss Software for Building Damage Estimation

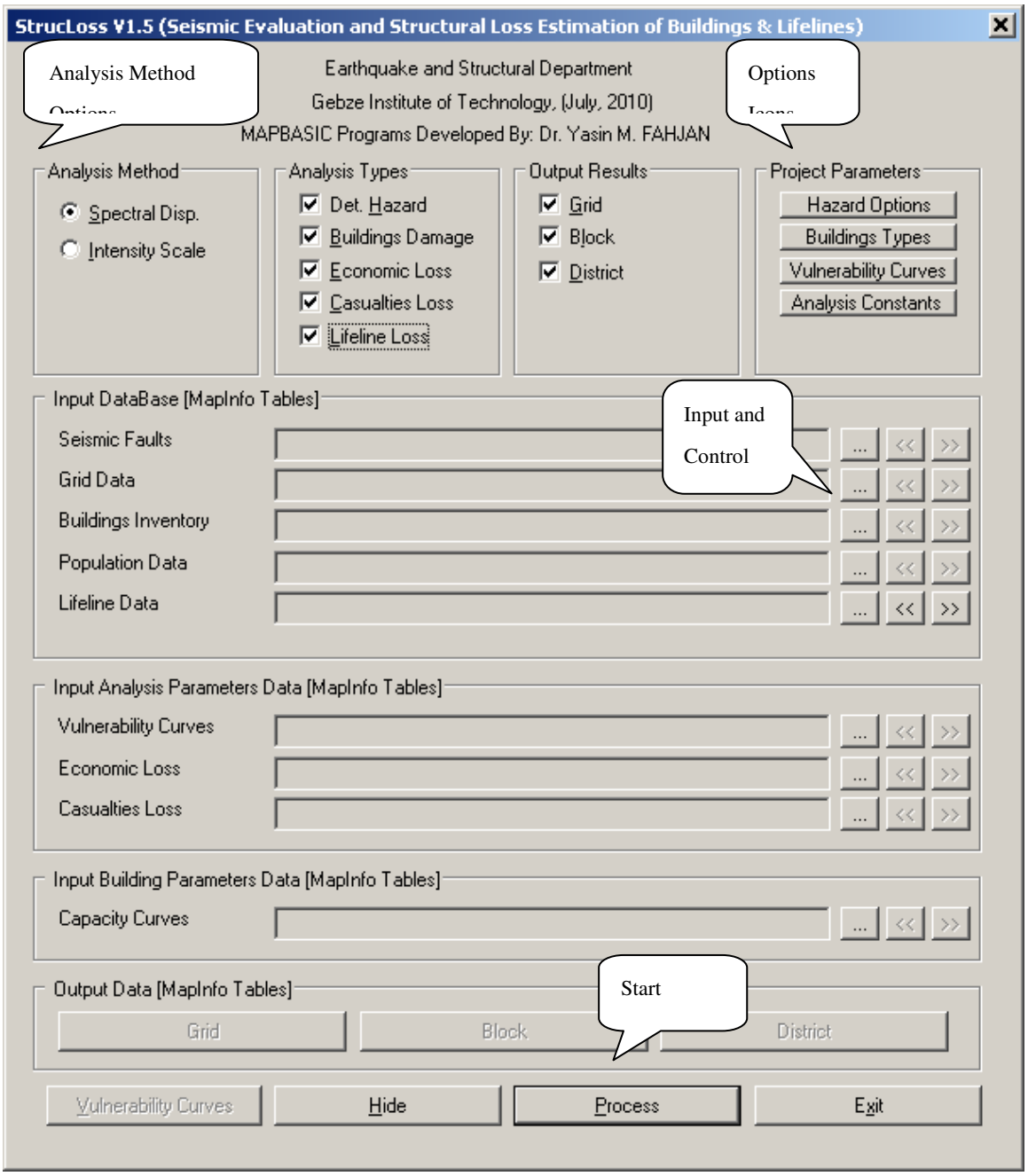

StrucLoss 1.5 Main Window Dialog

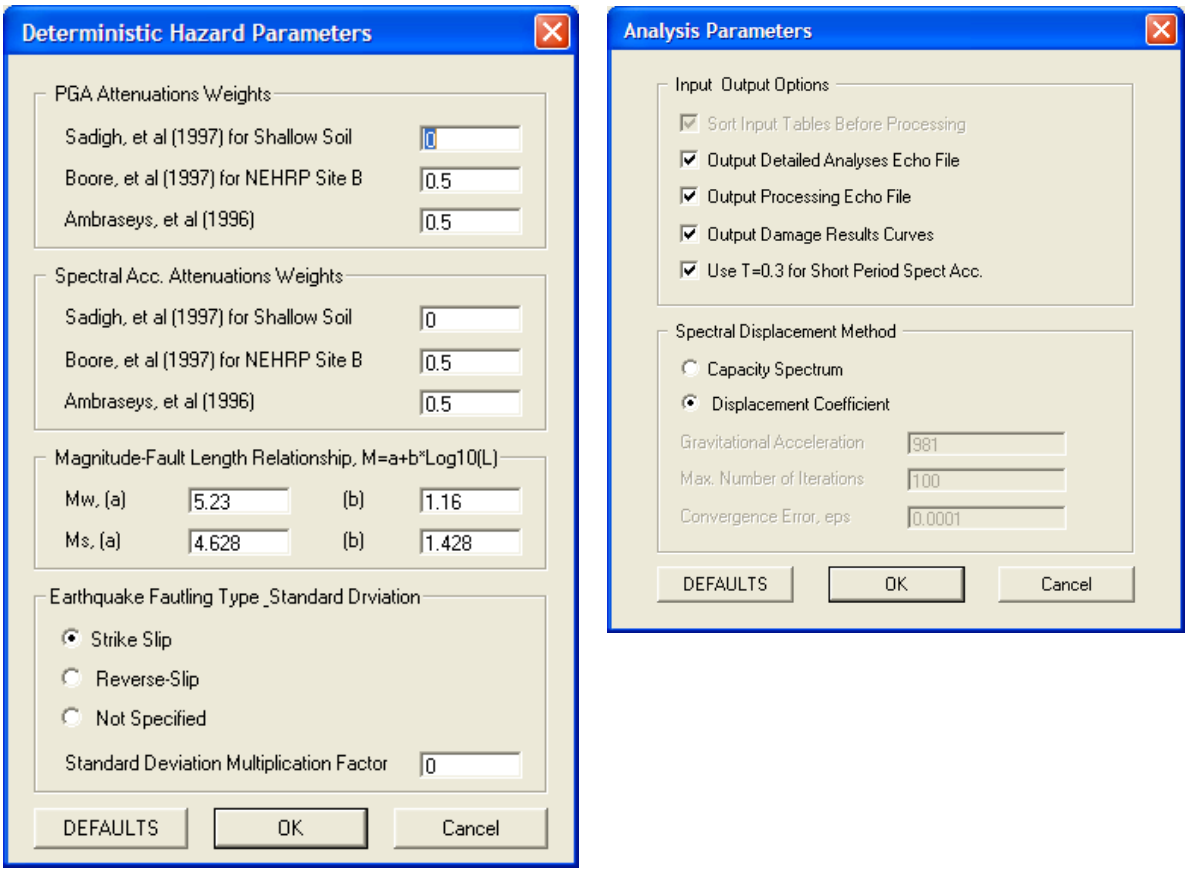

Dialog Form for Deterministic Hazard and Analyses Parameters

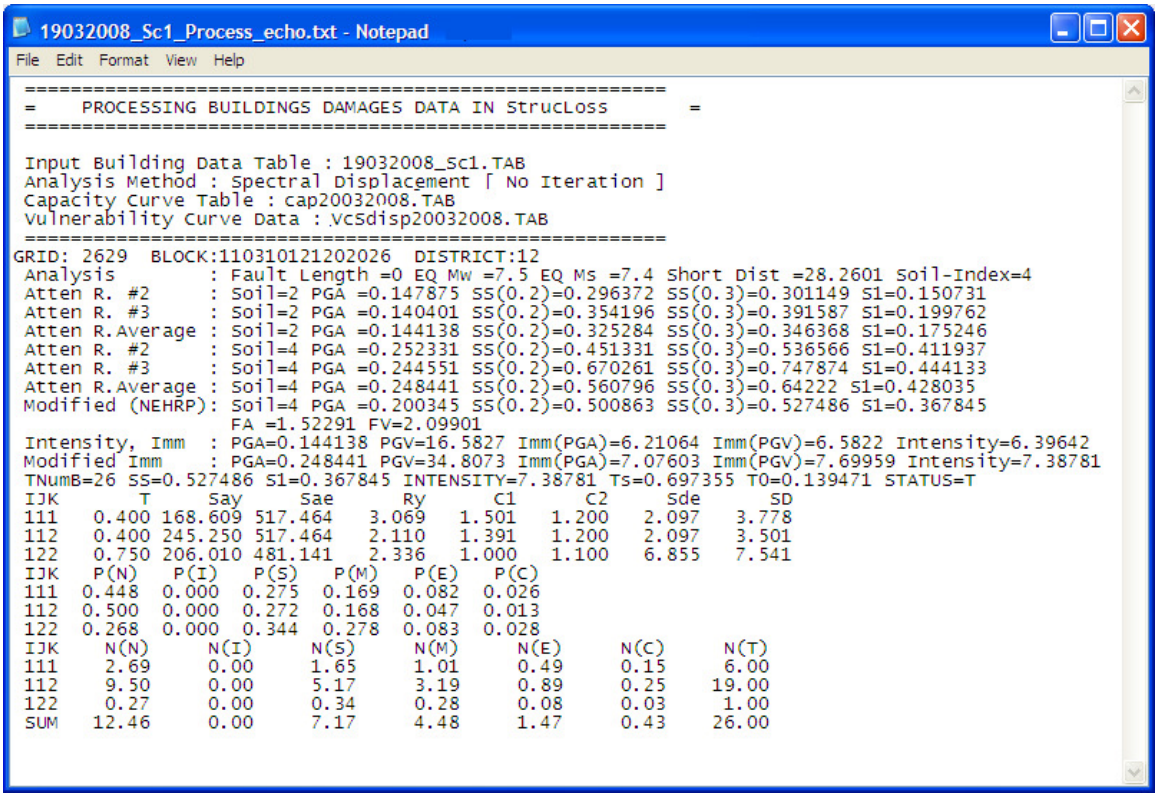

Detailed Output Control of the Analyses for Deterministic Hazard and Building Losses

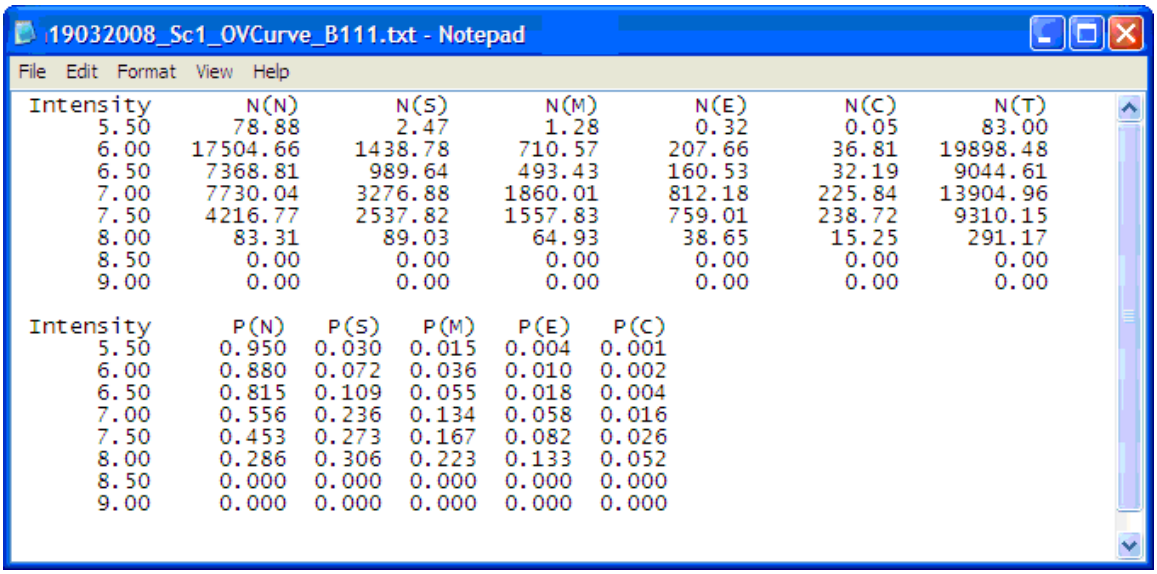

19032008_Sc1_OVCurve_B111.txt - Notepad

File Edit Format View Help

Intensity	N(N)	N(S)	N(M)	N(E)	N(C)	N(T)
5.50	78.88	2.47	1.28	0.32	0.05	83.00
6.00	17504.66	1438.78	710.57	207.66	36.81	19898.48
6.50	7368.81	989.64	493.43	160.53	32.19	9044.61
7.00	7730.04	3276.88	1860.01	812.18	225.84	13904.96
7.50	4216.77	2537.82	1557.83	759.01	238.72	9310.15
8.00	83.31	89.03	64.93	38.65	15.25	291.17
8.50	0.00	0.00	0.00	0.00	0.00	0.00
9.00	0.00	0.00	0.00	0.00	0.00	0.00

Intensity	P(N)	P(S)	P(M)	P(E)	P(C)
5.50	0.950	0.030	0.015	0.004	0.001
6.00	0.880	0.072	0.036	0.010	0.002
6.50	0.815	0.109	0.055	0.018	0.004
7.00	0.556	0.236	0.134	0.058	0.016
7.50	0.453	0.273	0.167	0.082	0.026
8.00	0.286	0.306	0.223	0.133	0.052
8.50	0.000	0.000	0.000	0.000	0.000
9.00	0.000	0.000	0.000	0.000	0.000

Intensity based outputs of the results for each damage states

Buildings Structural Capacity Estimation and Fragility Curves Validation

Buildings Structural Capacity and Fragility Curves Parameters Estimation

Comprehensive procedure based on Pushover analyses is considered to estimate the initial capacity curves and fragility curves parameters. The guidelines proposed in Chapters 5 and 6 of Hazus-MH-MR3 (2003) are followed when it is applicable. The estimation methodology can be summarized as follows

- The buildings dimensions and detailing are based on average values for real buildings designed and constructed by local engineering experience in Aqaba. The details of the buildings used in the analyses are given below.
- The skeleton type building is a type of R/C Moment Frame. The local engineer called it skeleton type because all the analyses and computations for the design forces are based on continuous beams theory or approximate Hardy Cross's moment distributions. The standard R/C Moment Frame detailing of beams and columns are applied but with the lack of shear confinement at the beam-columns joints.
- In 1990's the engineering supervision for buildings and concrete quality were greatly improved. This change influence a better design practice and engineering controls. In this project we consider 1990 as the year of change.
- The pushover analyses are performed for typical buildings with average dimensions and detailing. The analyses are done on typical representative building to initially estimate the capacity and fragility curves parameters. The initially estimated parameters were considerably updated using calibration process with the empirically based intensity data.
- The structural analyses software SAP2000 V14 is used to model and analyze the buildings structures. The Finite Element models and buildings details are plotted for each building class.
- Frame elements are used to model beams and columns, while main pier-rigid beam models are utilized for shear walls.

- The stiffness of brick based infill walls is ignored and their masses and weights are considered in the models.
- The stiffness of stone-concrete infill walls are considered based on the works of Royal Scientific Society, Building Research Center (2003) and Al-Nimry H S. (2010).
- The cracked section properties for beams and column are considered for modal and Pushover analyses.
- The hinge M3 properties for the beams and PMM hinges properties for the columns are computed based on FEMA 356 recommendations for concrete beams using the existing concrete type and reinforcing steel rebars.
- The hinge PMM properties for columns are based on FEMA 356 recommendations for the existing reinforcements details and the nonlinearity for the shear walls are considered as main pier-rigid beam system as explained in Fahjan et al (2010). A standard detailing of the shear walls are shown in Figure C1 below.
- The nonlinear behavior of stone-concrete infill walls are modeled using approximate nonlinear link model for old and new constructions as shown in Figure C.2 below. The nonlinear link models properties are computed based on the experimental works of Al-Nimry H S. (2010).
- The hinges for beams and columns are located at both ends of the members.
- To include the effect of soft stories in the buildings classes (B421, B422), the first floor are considered to be much higher than the upper stories. The stone-concrete infill walls are modeled using nonlinear link elements.
- To ensure a convergence in the analysis for the three dimensional models with many irregularities such as shear-walls elements and infill elements; the moment-rotation curve for the hinges is assumed to be elasto-plastic with no load drop. Even though, the approach may lead to monolithic increase in capacity, it has minimum effects on resulting plastic rotations and drift ratio. This approach is recommended in contemporary codes as Turkish Earthquake Code (2007).

- The Pushover capacity curves for each building type in both X and Y directions are given for each building class.
- The spectral yield acceleration, S_{ay}, estimated from pushover capacity curve is equivalent to ultimate capacity, A_u, defined in Hazus99.
- The building natural fundamental period is estimated from the modal (eigenvalues) analysis results of SAP2000. The average of X and Y directions are approximated.
- The fragility curve mean spectral displacement values are estimated by computing the drift ratio from the base shear-roof displacement of the pushover curve, utilizing the drift ratio proposed by Hazus MH (2003) to define Slight, Moderate, Extensive, Complete damage states. The drift ratios used to determine the mean spectral displacement are given in .4.12 for each building class together with the corresponding building type in HAZUS.
- The initial values of fragility curves Beta β (β_c ,$\beta_{T,ds}$) are utilized the values proposed in Hazus MH (2003) and those proposed in GAM.

Typical Drift Ratios Based on HAZUS-MH (2003) for Different Building Classes

Building Class	HAZUS Building Type	Slight	Moderate	Extensive	Complete
B111	C1-Low-Rise (Low Code)	0.005	0.008	0.020	0.050
B112	C1-Low-Rise (Low Code)	0.005	0.008	0.020	0.050
B121	C1-Mid-Rise ((Moderate Code)	0.003	0.006	0.015	0.040
B211	C1-Low-Rise (Low Code)	0.005	0.008	0.020	0.050
B212	C1-Low-Rise (Low Code)	0.005	0.008	0.020	0.050
B221	C1-Mid-Rise (Low Code)	0.003	0.005	0.013	0.033
B222	C1-Mid-Rise (Low Code)	0.003	0.005	0.013	0.033
B311	C1-Low-Rise (Moderate Code)	0.005	0.009	0.023	0.060
B321	C1-Mid-Rise ((Moderate Code)	0.003	0.006	0.015	0.040
B411	C1-Low-Rise (Low Code)	0.005	0.008	0.020	0.050
B421	C1-Mid-Rise (Low Code)	0.003	0.005	0.013	0.033
B422	C1-Mid-Rise (Low Code)	0.003	0.005	0.013	0.033
B512	C1-Low-Rise (Low Code)	0.005	0.008	0.020	0.050

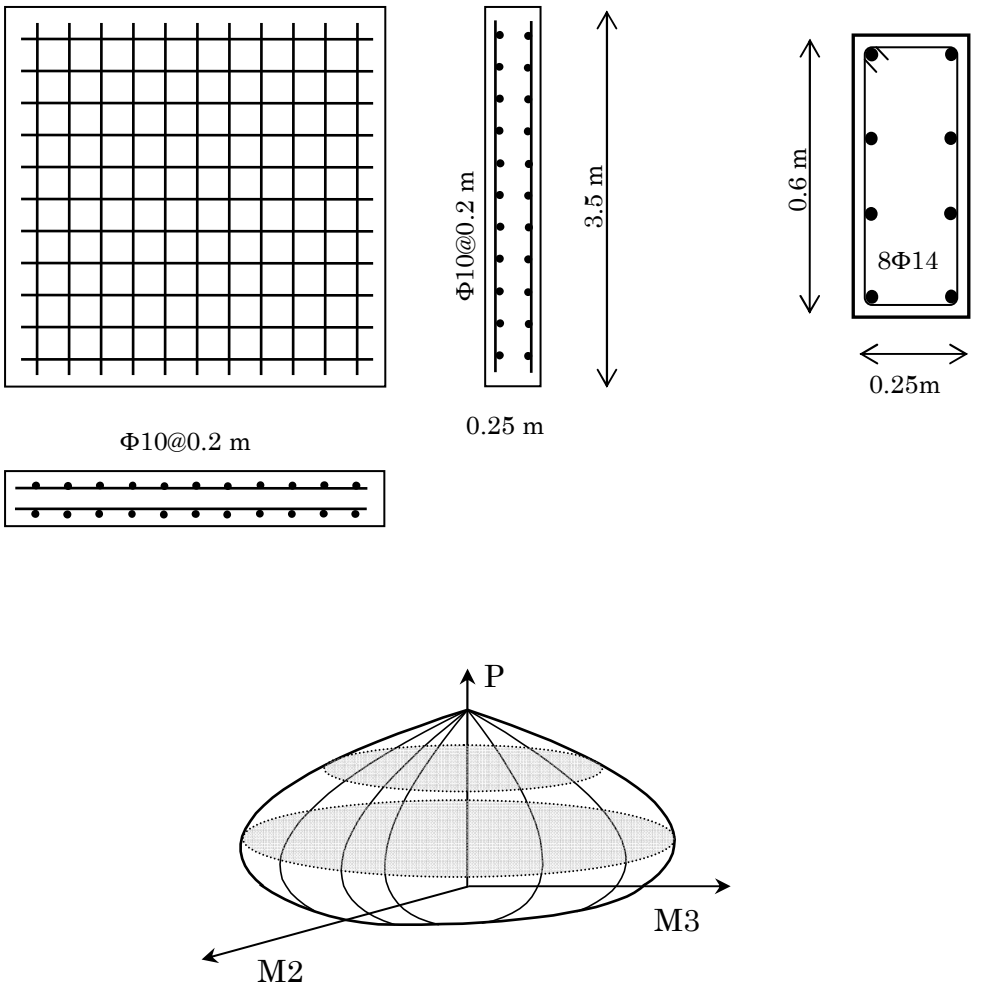

Figure C1: Example of reinforcement distribution in the shear wall and column members and PMM plastic hinge